ELSEVIER

Contents lists available at ScienceDirect

## Journal of Hydrology

journal homepage: www.elsevier.com/locate/jhydrol



## Research papers

# River flow decline across the entire Arkansas River Basin in the 21st century



Jia Yang a,\*, Chris Zou a, Rodney Will a, Kevin Wagner b, Ying Ouyang c, Chad King d, Abigail Winrich a, Hangin Tian e

- Department of Natural Resource Ecology and Management, Division of Agricultural Sciences and Natural Resources, Oklahoma State University, Stillwater, OK 74078, USA
- Oklahoma Water Resources Center, Division of Agricultural Sciences and Natural Resources, Oklahoma State University, Stillwater, OK 74078, USA CUSDA Forest Service, Center for Bottomland Hardwoods Research, 775 Stone Blvd., Thompson Hall, Room 309, MS State, MS 39762, USA Department of Biology, University of Central Oklahoma, 100 N. University Dr., Edmond, OK 73034, USA Schiller Institute for Integrated Science and Society, Department of Earth and Environmental Sciences, Boston College, Chestnut Hill, MA 02467, USA

#### ARTICLEINFO

"This manuscript was handled by Marco Borga, Editor-in-Chief, with the assistance of Eylon Shamir, Associate Editor"

Keywords:
Climate change
Hydrological modeling
Droughts
Surface runoff
Great plains
Evapotranspiration

#### ABSTRACT

The Arkansas River and its tributaries provide critical water resources for agricultural irrigation, hydropower generation, and public water supply in the Arkansas River Basin (ARB). However, climate change and other environmental factors have imposed significant impacts on regional hydrological processes, resulting in widespread ecological and economic consequences. In this study, we projected future river flow patterns in the 21st century across the entire ARB under two climate and socio-economic change scenarios (i.e., SSP2-RCP45 and SSP5-RCP85) using the process-based Dynamic Land Ecosystem Model (DLEM). We designed "baseline simulations" (all driving factors were kept constant at the level circa 2000) and "environmental change simulations" (at least one driving factor changed over time during 2001-2099) to simulate the inter-annual variations of river flow and quantify the contributions of four driving factors (i.e., climate change, CO<sub>2</sub> concentration, atmospheric nitrogen deposition, and land use change). Results showed that the Arkansas River flow in 2080-2099 would decrease by 12.1% in the SSP2-RCP45 and 27.9% in the SSP5-RCP85 compared to that during 2000-2019. River flow decline would occur from the beginning to the middle of this century in the SSP2-RCP45 and happen throughout the entire century in the SSP5-RCP85. All major rivers in the ARB would experience river flow decline with the largest percentage reduction in the western and southwestern ARB. Warming and drying climates would account for 77%-95% of the reduction. The rising CO<sub>2</sub> concentration would exacerbate the decline through increasing foliage area and ecosystem evapotranspiration. This study provides insight into the spatial patterns of future changes in water availability in the ARB and the underlying mechanisms controlling these changes. This information is critical for designing watershed-specific management strategies to maintain regional water resource sustainability and mitigate the adverse impacts of climate changes on water availability.

## 1. Introduction

The Arkansas River is one of the major tributaries of the Mississippi River,

endangered aquatic species. However, as a prevalent land disturbance in the ARB (Basara et al., 2013), droughts disrupt the normal hydrological processes, reduce water availability in rivers and lakes, and cause widespread ecological

Received 4 October 2022; Received in revised form 26 January 2023; Accepted 5 February 2023 Available online 8 February 2023

0022-1694/© 2023 Elsevier B.V. All rights reserved.

originating in the Rocky Mountains in New Mexico and Colorado, flowing through the plains and highlands in Kansas and Oklahoma, and finally joining the Mississippi River in Arkansas. The Arkansas River Basin (ARB) is the largest river basin in the southern Great Plains spanning a large diversity of climate, terrain, and vegetation. River flow in the Arkansas River and its tributaries provide critical water resources for agricultural irrigation, hydropower generation, and public water supply and provide habitats for several

consequences and agricultural and economic losses (Seager et al., 2013). Many rivers in the ARB flow across the boundary of multiple states, which requires interstate stream compacts to apportion the waters and resolve conflicts between states (Schlager and Heikkila, 2009).

In the ARB, the surface water in rivers and lakes is an essential source for agriculture irrigation and public water supply. Diversion facilities

<sup>\*</sup> Corresponding author at: 008 Ag Hall, Department of Natural Resource Ecology and Management, Oklahoma State University, Stillwater, OK 74078, USA. *E-mail address*: jia.yang11@okstate.edu (J. Yang). https://doi.org/10.1016/j.jhydrol.2023.129253

were constructed in Colorado between Avondale and La Junta to remove water from the Arkansas River for irrigation use and substantially decreased streamflow (Gates et al., 2016; Ortiz et al., 1998). In Oklahoma, daily surface water withdrawals reached 989 million gallons in 2005, 32 % of which was used for cropland irrigation (Tortorelli, 2009). Additionally, a number of important U.S. cities reside along the Arkansas River and its tributaries, including Oklahoma City and Tulsa in Oklahoma, Little Rock in Arkansas, Wichita in Kansas, and Pueblo in Colorado. With the increasing urban population, surface water has become the primary public water supply source in the eastern ARB. In Kansas, surface water represented 52–61 % of the total annual withdrawals for public supply during 1990-2012 (Kenny, 2014). In Oklahoma, 41 % of the surface water withdrawals have been used as public water supply. Additionally, the Arkansas River and its tributaries provide critical habitats for multiple endangered aquatic species. For example, the Arkansas River shinner is endemic to the Arkansas River system, but its abundance and living extent started to shrink in the 1970s (Pigg, 1999).

The southern Great Plains and the ARB are prone to various types of droughts (multiyear droughts, seasonal droughts, and flash droughts) with severe consequences to regional water availability, crop production, and livestock health (Livneh and Hoerling, 2016). The southern Great Plains has experienced a number of multiyear droughts, such as the droughts in the 1930s and the 1950s, when sea surface temperatures in the tropics were lower than normal (Schubert et al., 2004). Seasonal droughts were prevalent in the ARB in the 20th century and the early 21st century and will likely become more frequent and severe after the 2050s along with climate warming and drying (Liu et al., 2013a). Over recent years, flash droughts at the sub-seasonal timescale have been intensively investigated in the U.S. (e.g. Basara et al., 2019; Chen et al., 2019; Christian et al., 2019). The ARB and the central Great Plains have been identified as hot spots with the most intense flash droughts, such as the Great Plain drought in 2011 (Christian et al., 2019). These drought events decreased river flow and surface water storage. For example, the water level in Lake Thunderbird in central Oklahoma was 7 feet (about 2.1 m) below the recommended conservation pool during the 2011/2012 drought, threatening the drinking water supply in the three metropolitan areas of Midwest City, Del City, and Norman. Another drastic example is Lake Meredith on the Canadian River, which historically was a major source of drinking water for cities in the Texas Panhandle. By 2012, however, the lake level has dropped to the point that no water was delivered to these cities (Cepeda, 2016). Additionally, some reaches of the Arkansas River (such as that between Dodge City and Garden City in Kansas) were once perennial, but completely dry over recent decades.

Due to the limited water resources over a large portion of the ARB, disputes regarding river water apportionment have long been common between neighboring states (Clemons, 2003). For example, water conflicts between Kansas and Colorado over the apportionment of Arkansas River flows happened multiple times since the early 20th century. From 1950 to 1985, Colorado intercepted 328,000 acre-feet of Arkansas River water that was supposed to flow to Kansas (Naeser and Bennett, 1998). Kansas sued Colorado in the U.S. Supreme Court that Colorado deprived Kansas of its accustomed flow of the Arkansas River. To manage and apportion the waters in the Arkansas River and its major tributaries, many interstate stream compacts have been approved by the United States Congress and enacted in Federal statutes and the statutes of each agreeing State (Schlager and Heikkila, 2009). To design better strategies for surface water allocation, information regarding future river flow is urgently needed by the States in the ARB.

Climate change has affected and will continue altering river hydrological regimes and endanger water resource sustainability at the regional and global scales (Seager et al., 2013; van Vliet et al., 2013). Quantitative information about future river flow under climate change and water use scenarios is of particular importance for water risk assessment (Nohara et al., 2006) and designing proactive intervention water management strategies (Palmer et al., 2008). Future climate change will likely worsen water shortages in the ARB by enhancing water demand while reducing water supply. Changed precipitation regimes will affect soil moisture conditions and runoff generation (Seager et al., 2013). Climate warming will likely increase ecosystem evapotranspiration and in turn drive up irrigation water requirements and public water use (Yang

et al., 2019a). Additionally, ecosystem evapotranspiration and river flow can be affected by many other environmental factors. For example, Tao et al. (2014) reported that under the high-emission scenarios, human-induced rising CO<sub>2</sub> concentration and land-use change would play a more important role than climate change in shaping the river discharge of the Mississippi River. In contrast, Piao et al. (2007) found that climate change and cropland expansion had a larger impact than the rising CO<sub>2</sub> concentrations in determining river flow trend. One critical pattern of land cover change in the ARB is woody plant encroachment in the grasslands, which has been found to affect runoff generation and groundwater recharge (Acharya et al., 2018; Qiao et al., 2017). It can be concluded that an accurate simulation of future river flow needs to consider the impacts of climate change as well as other human-caused environmental changes. Although future river flow has been projected in many basins in the U.S. and across the world under climate change scenarios (e.g. Lauri et al., 2012; Seager et al., 2013; Tao et al., 2014), we lack an in-depth understanding of future river flow patterns in the ARB and the southern Great Plains, which is limiting our ability to design water use and management strategies to sustain regional water resource availability.

In this study, we aimed at answering the following two questions: (1) How much would river flow change over different parts of the ARB in the middle and at the end of the 21st century? (2) What are the major environmental factors controlling future river flow changes? To answer these two questions, we compiled and analyzed future projections of climate conditions and other environmental factors from the Coupled Model Intercomparison Project Phase 5 and Phase 6 (CMIP5 and CMIP6) and used these compiled future environmental factors to drive the process-based Dynamic Land Ecosystem Model (DLEM, Tian et al. (2011)). We designed "baseline simulations" (all driving factors were kept constant at the level circa 2000) and "environmental change simulations" (at least one driving factor changed over time during 2001–2099) to simulate the inter-annual variations of river flow in the ARB and quantify the contributions of four driving factors (i.e., climate change, CO<sub>2</sub> concentration, atmospheric nitrogen deposition, and land use change). Contrasting to previous river flow modeling studies that report river flow at one or multiple river outlets, our work presented the spatial pattern of future river flow of all major river channels in the ARB, which is critical for designing water management strategies at the local, state, and basin levels.

## 2. Data and methods

## 2.1. Study domain

Our study domain is the Arkansas River Basin (Fig. 1), which has a total land area of 0.41 million km² and covers parts of 7 states (Colorado, New Mexico, Kansas, Oklahoma, Texas, Missouri, and Arkansas) and 16 EPA Level III Ecoregions (Fig. S1). We delineated the ARB boundary based on the Hydro1k Digital Elevation Model (DEM) data using hydrological analysis tools in ArcGIS 10.8. We identified the major river channels (Fig. 1) from the Hydro1k DEM by calculating flow accumulation area and then selecting grids with flow accumulation area > 16,000 km². Topography presents significant spatial variations in the east—west direction (Fig. S2). The ecoregion of the Mississippi Alluvial Plain in Arkansas (see its location in Fig. S1) has the lowest elevation (mean = 61 m), while the ecoregion of the Southern Rockies in Colorado and New Mexico has the highest elevation (mean = 2636 m).

According to the gridMet climate data (Abatzoglou, 2013), ARB had an average annual temperature of 8.4 °C during 1991–2020 with the highest

accounting for 42.5 % of the entire ARB land area. Forest and shrub are the second and third largest natural vegetation types, representing 14.7 % and 13.2

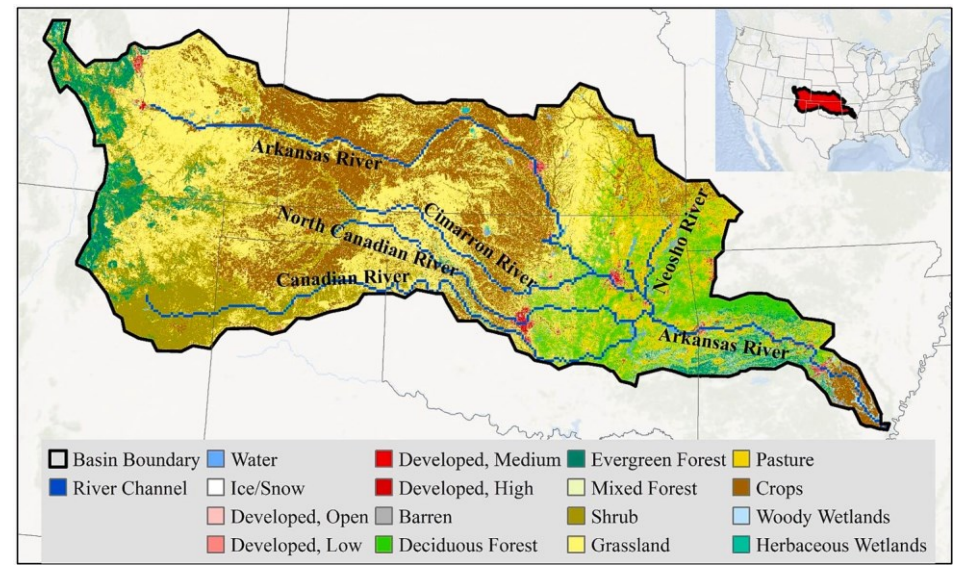
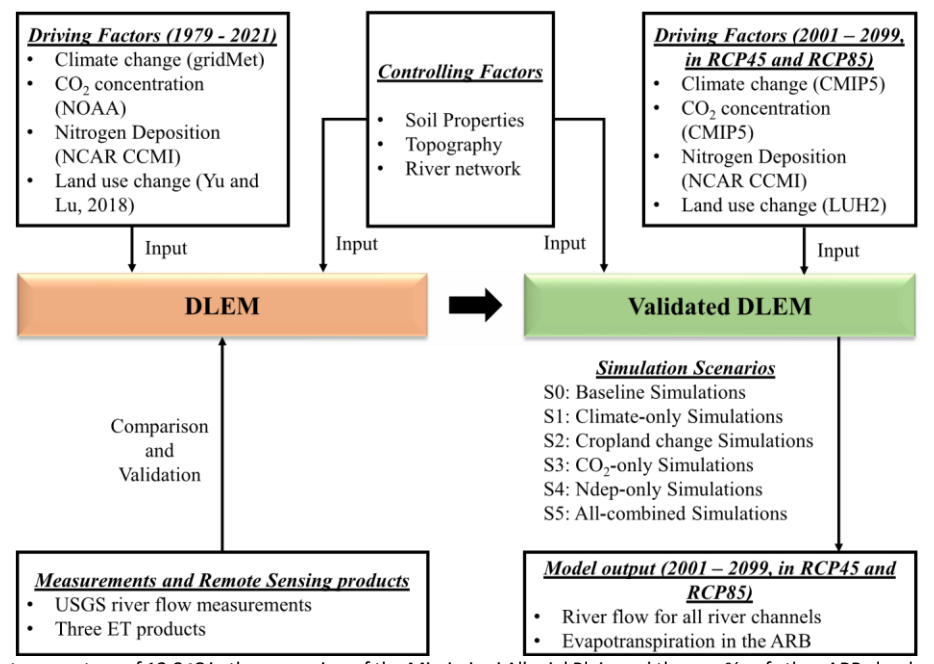


Fig. 1. Study domain of the Arkansas River Basin (ARB), major river channels, and land cover types. Inset shows the location of the ARB in the U.S.



**Fig. 2.** Flowchart of methodology to simulate river flow in the Arkansas River Basin (ARB) during 2001–2099 in model simulation scenarios. Abbreviations in this figure: DLEM – Dynamic Land Ecosystem Model, NOAA – National Oceanic and Atmospheric Administration, NCAR – National Center for Atmospheric Research, CCMI – Chemistry-Climate Model Initiative, CMIP5 – Coupled Model Intercomparison Project, phase 5, LUH2 – Land-Use Harmonization data, and RCP – Representative Concentration Pathways.

temperature of 12.2 °C in the ecoregion of the Mississippi Alluvial Plain and the lowest temperature of 1.2 °C in the ecoregion of the Southern Rockies (Fig. S3). July was the warmest month (20.7  $\pm$  2.8 °C, mean  $\pm$  1 std. dev., same hereafter), and January was the coldest month (-3.6 ± 2.1 °C, Fig. S4). During the last 30 years, regional average precipitation was 732 mm/year with a distinct declining pattern from east to west. May was the month with the highest precipitation (94.7 ± 56.3 mm/month), and January was the month with the lowest precipitation (28.4  $\pm$  27.9 mm/month, Fig. S4). The average potential evapotranspiration was 1490 mm/year for the ARB. Potential evapotranspiration was the highest in the southwestern ARB (>1700 mm/year). As an indicator of aridity conditions, the aridity index (AI, the ratio of long-term precipitation to long-term potential evapotranspiration) (Middleton and Thomas, 1998) was 0.49 in the ARB with a large spatial variation from less than 0.3 in the arid west to>1.0 in the humid east. The dryland area (AI less than 0.65) accounted for 69.7 % of the ARB and the humid area (AI ≥ 0.65) accounted for the remaining 31.3 %.

As shown by the National Land Cover Database 2019 (Fig. 1, Homer et al., 2020), grassland and pasture are the dominant land use and land cover types,

% of the ARB land area, respectively. Deciduous forests are primarily distributed in the eastern ecoregions, such as the Cross Timbers, the Boston Mountains, the Arkansas Valley, and the Ozark Highlands (see their locations in Fig. S1). Evergreen forests are prevalent in the ecoregion of the Southern Rockies in the west. Croplands account for 22.5 % of the ARB land area, mostly occurring in the ecoregions of the High Plains, the Central Great Plains, and the Mississippi Alluvial Plain.

#### 2.2. Model description and experimental design

In this study, we first evaluated the performance of Dynamic Land Ecosystem Model (DLEM) in simulating evapotranspiration and river flow in the ARB against USGS measurement and satellite-based evapotranspiration products. After model evaluation and validation, we ran the validated DLEM to simulate the annual river flow from 2001 to 2099 in six model simulation scenarios. Model driving forces included climate change, CO<sub>2</sub> concentration, atmospheric nitrogen deposition, and land use change (Fig. 2).

#### 2.2.1. Dynamic land ecosystem model

DLEM is a process-based ecosystem model for simulating ecosystem water, carbon, and nitrogen processes at the site, regional, and global scales (Liu et al., 2013b; Tian et al., 2011; Yao et al., 2020). The terrestrial processes include five major components, including biophysical, biogeochemical, hydrological, vegetation dynamics, and land- use processes (Tian et al., 2010). In the ARB, DLEM includes seven major Plant Functional Types (PFTs) to represent the distribution of natural vegetation, which are temperate broadleaf deciduous forest, temperate needleleaf evergreen forest, evergreen shrub, deciduous shrub, C3 grass, C4 grass, and wetland. In each grid, DLEM uses a cohort structure to represent land cover types with a maximum of four natural vegetation PFTs and one crop type (Liu et al., 2013b). Natural and anthropogenic land disturbances, such as wildfires, forest harvesting, and herbivore grazing, have been explicitly represented, enabling DLEM to simulate the impacts of anthropogenic and natural disturbances on ecosystem carbon and water dynamics (Chen et al., 2013; Dangal et al., 2017; Yang et al., 2015a). DLEM also has the capability to evaluate land-use change and land management practices (such as fertilizer application and timber harvest) on the terrestrial and aquatic processes (Lu et al., 2020; Pan et al., 2021; Ren et al., 2016; Tian et al., 2020; Yang et al., 2015b). The aquatic module in DLEM simulates sub-grid-level hydrological processes as well as water, nutrient, and sediment transport between grids through river networks down to the ocean. It is unique in the incorporation of various environmental drivers, simultaneous simulations of terrestrial water/carbon/nitrogen dynamics, land-toatmosphere gas and water exchanges, and land-to-aquatic mass flows (Tian et al., 2020; Yao et al., 2020). Text S1 provides a brief description of DLEM algorithms to estimate ET, runoff, baseflow, and water movement along the river network. The detailed description can be found in our previous publications (Liu et al., 2013b; Pan et al., 2015; Yang et al., 2015b; Yao et al., 2020).

#### 2.2.2. Model input datasets

In this study, we prepared model input datasets at a spatial resolution of 4-km, which is the highest resolution for the downscaled CMIP5 future climate data in the ARB. The static model input variables included soil properties, topography, and river network. We obtained soil property data from the gridded Harmonized World Soil Database (HWSD) v1.2 (Wieder, 2014), including soil texture, pH value, and bulk density. Next, we used the Arc Hydro Tools in ArcGIS (Djokic et al., 2011) to fill sinks in the Hydro1k DEM data, calculate flow direction and accumulation area, determine river channels, and delineate basin boundary.

Time-varying model inputs include daily climate conditions, CO<sub>2</sub> concentration, atmospheric nitrogen deposition, and annual cropland distribution. Climate data (daily average/maximum/minimum air temperature, precipitation, and solar radiation) were from two data sources, i.e., the 4-km gridMet climate data from 1979 to 2021 (Abatzoglou, 2013) and downscaled General Circulation Model (GCM) outputs in the CMIP5 project over the historical period (1980-2005) and future period (2006-2099) in two Representative Concentration Pathways with medium and high greenhouse gas concentrations, i.e., RCP45 and RCP85 scenarios (Taylor et al., 2012). We used CMIP5 climate data from seven GCMs, which are BCC-CSM1, CCSM4, GFDL-ESM2G, HadGEM2-ES365, IPSL-CM5A-LR, MIROC5, and NorESM1-M. These data have been downscaled to a spatial resolution of 4-km and bias has been corrected according to the gridMet historical climate data using the Multivariate Adaptive Constructed Analogs (MACA) (Abatzoglou and Brown, 2012). It is noteworthy that we used the downscaled climate data from the CMIP5 rather than the CMIP6, although downscaled CMIP6 climate data are available (such as the NEX-GDDP-CMIP6, Thrasher and Nemani (2021)). This is because the spatial resolution of current CMIP6 downscaled climate data (such as 0.25° latitude/longitude for the NEX-GDDP-CMIP6) is not high enough to meet our requirement for hydrological simulations in the ARB.

Annual  $CO_2$  concentration data between 1979 and 2020 were from the NOAA Global Monitoring Laboratory and future  $CO_2$  concentration data in the RCP45 and RCP85 scenarios were obtained from the RCP database version 2.0. The atmospheric nitrogen deposition data (NHx and NOy, 0.5°

latitude/longitude) in the historical and future periods were from the NCAR Chemistry-Climate Model Initiative (CCMI), which has been used in the Global  $N_2O$  Model Intercomparison Project (NMIP, Tian et al. (2018)). These nitrogen deposition data were simulated by atmospheric chemistry models in scenarios combining Shared Socioeconomic Pathways (SSP) and RCP, i.e., SSP2-RCP45 and SSP5-RCP85. In this study, we further downscaled these data to a spatial resolution of 4-km using the bilinear interpolation method to drive DLEM.

To construct the future distribution of cropland and natural vegetation, we first developed a 30-m natural vegetation land cover map by replacing cropland pixels in the NLCD 2019 with their nearest natural vegetation/land cover pixels. Next, we downloaded the 1-km historical fractional cropland data (1979–2016) developed by Yu and Lu (2018) and extracted future fractional cropland data (2015–2099) in the SSP2- RCP45 and SSP5-RCP85 scenarios from the Land-Use Harmonization data (LUH2, Hurtt et al. (2020)). We modified cropland fractions in the LUH2 based on cropland fractions in the Yu and Lu (2018) dataset to make cropland fractions in the two datasets connect seamlessly. Finally, we overlayed the annual cropland fraction datasets on the 30-m natural vegetation land cover map and computed the fractions of vegetation types in each 4-km grid for model simulations during 1979–2099. The major crop types in the ARB include winter wheat, soybean, corn, sorghum, and hay.

#### 2.2.3. Model validation and result comparison

In this study, DLEM simulations consisted of two stages, which were the equilibrium run and the transient run. In the equilibrium run stage, the model was driven by the 20-year average climate condition between 1979 and 1998 from gridMet. The other driving factors (cropland distribution, atmospheric nitrogen deposition, and  $CO_2$  concentration) were kept constant at the level in 1979. Vegetation seeds started to grow from the bare ground with no soil carbon, nitrogen, and water storage until the system reached an equilibrium state, defined as the changes in grid-level ecosystem carbon, nitrogen, and water storage between two consecutive 20-year periods less than  $0.5 \text{ g C} / \text{m}^2$ ,  $0.5 \text{ g N} / \text{m}^2$ , and  $0.5 \text{ g H}_2\text{O} / \text{m}^2$ , respectively. For most simulation grids in the ARB, it took 1,000-10,000 years for the model to reach an equilibrium state.

Next, we implemented model validation and result comparison by designing the transient run from 1979 to 2021 driven by gridMet climate data and other time-varying driving forces. The transient run used the simulated carbon, water, and nitrogen status in the equilibrium run as the starting point. DLEM parameters controlling ecosystem evapotranspiration and water yield processes (such as leaf stomatal conductance and soil surface reflectance) were from Pan et al. (2015), which have been validated against ET measurements at 21 AmeriFlux sites in the U.S. We obtained other model parameters not directly related to ecosystem water processes from our recent simulations in the Inter- Sectoral Impact Model Intercomparison Project phase 2a (Pan et al., 2020; Shi et al., 2021). Then, these parameters were used to drive DLEM in the equilibrium run and the transient runs.

We compared DLEM-simulated monthly ET against the data-based latent heat product of Model Tree Ensembles (MTE, Jung et al. (2011)), ET estimates from the Global Land Evaporation Amsterdam Model (GLEAM, Martens et al. (2017)), and MODIS ET product of MOD16A3 (Mu et al., 2011). MTE ET was available from 1982 to 2011, GLEAM ET were available from 2003 to 2020, and MODIS ET was available from 2001 to 2021. In this study, we compared DLEM ET with these three ET datasets from 2003 to 2011, during which all these datasets are available. Also, we compared model simulations of river flow against USGS measurements at five gauge stations along the Arkansas River and its major tributaries, including the site at Chouteau, OK (ID: 07191500, Neosho River), the site at Muskogee, OK (ID: 07194500, Arkansas River), the site at Murray Dam, AR (ID: 07263450, Arkansas River), the site at White Field, OK (ID: 07245000, Canadian River), and the site at Fort Smith, AR (ID: 07249455, Arkansas River). The locations of the five sites and their associated watersheds are illustrated in Fig. S5.

We used two goodness-of-fit metrics, i.e., the Nash-Sutcliffe Efficiency (NSE, Nash and Sutcliffe (1970)) and percent bias (PBIAS, Gupta

Table 1

et al. (1999)), to evaluate DLEM's performance in simulating monthly river flow. NSE is a normalized statistic metric that quantifies the relative magnitude of the residual variance compared to the variance of river flow measurements, ranging from -∞ to 1.0 with NSE = 1 being the perfect simulation and NSE > 0 as acceptable levels of performance (Moriasi et al., 2007). PBIAS measures the tendency of DLEM-simulated river flow to be larger or smaller than the measurements with PBIAS = 0 being the perfect simulation and a lower absolute value of PBIAS indicating a more accurate simulation (Moriasi et al., 2007). Positive PBIAS values indicate model underestimates river flow, while negative values indicate overestimation.

Driving factors for DLEM transient runs and model simulation scenarios (SO to S5) in the period of 2001–2099.

\$0: Baseline Simult  2  3  4  5  6  7  8  9  10  11  12  13  14  15  \$S1: Climate-only  16  17  18  19  10  21  22  23  24  25	nulations S0.gridMet S0.BCC.RCP45 S0.BCC.RCP85 S0.CCSM4.RCP45	1981–2000 average			
1 2 3 4 4 5 5 5 6 7 7 8 8 9 10 11 12 12 13 14 15 S1: Climate-only 16 17 18 19 10 21 22 23 24	SO.gridMet SO.BCC.RCP45 SO.BCC.RCP85	1981–2000 average			
0 1 2 3 4 5 <b>S1:</b> Climate-only 6 17 18 19 10 21 22 23 24	SO.BCC.RCP45 SO.BCC.RCP85	1981–2000 average			
0 1 2 3 4 5 <b>S1:</b> Climate-only 6 17 18 19 10 21 22 23 24	SO.BCC.RCP85		2000	2000	2000
0 1 2 3 4 5 <b>51:</b> Climate-only 6 17 18 19 10 21 22 23 24		1981–2000 average	2000	2000	2000
1 2 3 4 4 5 5 51: Climate-only 5 17 18 19 10 21 22 23 24	SO CCSM4 RCP45	1981–2000 average	2000	2000	2000
1 2 3 4 4 5 5 51: Climate-only 5 17 18 19 10 21 22 23 24	JULICIJIVIT.INCI TJ	1981–2000 average	2000	2000	2000
1 2 3 4 4 5 5 51: Climate-only 5 17 18 19 10 21 22 23 24	S0.CCSM4.RCP85	1981–2000 average	2000	2000	2000
1 2 3 4 4 5 5 51: Climate-only 5 17 18 19 10 21 22 23 24	S0.GFDL.RCP45	1981–2000 average	2000	2000	2000
1 2 3 4 4 5 5 51: Climate-only 5 17 18 19 10 21 22 23 24	SO.GFDL.RCP85	1981–2000 average	2000	2000	2000
1 2 3 4 4 5 5 51: Climate-only 5 17 18 19 10 21 22 23 24	S0.HadGEM2.RCP45	1981–2000 average	2000	2000	2000
1 2 3 4 4 5 5 51: Climate-only 5 17 18 19 10 21 22 23 24	S0.HadGEM2.RCP85	1981–2000 average	2000	2000	2000
2 3 4 5 51: Climate-only 5 17 18 19 10 21 22 23 24	SO.IPSL.RCP45	1981–2000 average	2000	2000	2000
3 4 5 5 51: Climate-only 5 1 17 18 19 10 21 22 23 24	SO.IPSL.RCP85	1981–2000 average	2000	2000	2000
5 51: Climate-only 5 17 18 19 10 21 22 23 24	S0.MIROC5.RCP45	1981–2000 average	2000	2000	2000
55: Climate-only 51: Timate-only 517 18 19 10 21 22 23 24	S0.MIROC5.RCP85	1981–2000 average	2000	2000	2000
51: Climate-only 5 17 18 19 10 21 22 23 24	S0.NorESM1.RCP45	1981–2000 average	2000	2000	2000
5 17 18 19 10 21 22 23 24	S0.NorESM1.RCP85	1981–2000 average	2000	2000	2000
17 18 19 10 21 22 23 24	y Simulations				
18 19 10 21 22 23 24	S1.BCC.RCP45	2001–2099	2000	2000	2000
19 10 21 22 23 24	S1.BCC.RCP85	2001–2099	2000	2000	2000
19 10 21 22 23 24	S1.CCSM4.RCP45	2001–2099	2000	2000	2000
21 22 23 24	S1.CCSM4.RCP85	2001–2099	2000	2000	2000
21 22 23 24	S1.GFDL.RCP45	2001–2099	2000	2000	2000
23 24	S1.GFDL.RCP85	2001–2099	2000	2000	2000
23 24	S1.HadGEM2.RCP45	2001–2099	2000	2000	2000
24	S1.HadGEM2.RCP85	2001–2099	2000	2000	2000
	S1.IPSL.RCP45	2001–2099	2000	2000	2000
	S1.IPSL.RCP85	2001–2099	2000	2000	2000
26	S1.MIROC5.RCP45	2001–2099	2000	2000	2000
27	S1.MIROC5.RCP85	2001–2099	2000	2000	2000
28	S1.NorESM1.RCP45	2001–2099	2000	2000	2000
29	S1.NorESM1.RCP85	2001–2099	2000	2000	2000
S2: CC-only Simul		2001 2033	2000	2000	2000
)	S2.SSP2-RCP45	1981–2000 average	2001–2099	2000	2000
- [	S2.SSP5-RCP85	1981–2000 average	2001–2099	2000	2000
S3: CO <sub>2</sub> -only Simi					
2	S3.RCP45	1981–2000 average	2000	2001–2099	2000
3	S3.RCP85	1981–2000 average	2000	2001–2099	2000
S4: Ndep-only Sir					
4	S4.SSP2-RCP45	1981–2000 average	2000	2000	2001–2099
5	S4.SSP2-RCP85	1981–2000 average	2000	2000	2001–2099
S5: All-combined					
5	S5.BCC.SSP2-RCP45	2001–2099	2001–2099	2001–2099	2001–2099
7	S5.BCC.SSP5-RCP85	2001–2099	2001–2099	2001–2099	2001–2099
3	S5.CCSM4.SSP2-RCP45	2001–2099	2001–2099	2001–2099	2001–2099
)	S5.CCSM4SSP5-RCP85	2001–2099	2001–2099	2001–2099	2001–2099
, )	S5.GFDL.SSP2-RCP45	2001 2003	2001–2099	2001 2033	2001 2099
L	S5.GFDL.SSP5-RCP85	2001–2099	2001–2099	2001–2099	2001–2099
2	S5.HadGEM2.SSP2-RCP45	2001–2099	2001–2099	2001–2099	2001–2099
3	S5.HadGEM2.SSP5-RCP45	2001–2099	2001–2099	2001–2099	2001–2099
4	S5.IPSL.SSP2-RCP45	2001–2099	2001–2099	2001–2099	2001–2099
5	S5.IPSL.SSP5-RCP85	2001–2099	2001–2099	2001–2099	2001–2099
5			2001–2099	2001–2099	2001–2099
7	S5.MIROC5.SSP2-RCP45	2001–2099			
	S5.MIROC5.SSP5-RCP85	2001–2099	2001–2099	2001–2099	2001–2099
8 9	S5.NorESM1.SSP2-RCP45 S5.NorESM1.SSP5-RCP85	2001–2099 2001–2099	2001–2099 2001–2099	2001–2099 2001–2099	2001–2099 2001–2099

Note: "1981–2000 average", "2000", and "2001–2099" refer to the status of the four driving forces in model simulation period of 2001–2099. "1981–2000 average" indicates that driving forces were kept constant at the level of average conditions in 1981–2099. "2000" indicates that driving forces were kept constant at the level in 2000. "2001–2099" indicates that driving forces changed over time.

#### 2.2.4. Design of model simulations

Besides the transient run in 1979–2021 for model validation and result comparison (section 2.2.3), we designed another 49 model simulations in the period of 1979–2099 (Table 1). All the 49 simulations used the simulated carbon, water, and nitrogen status in the equilibrium run as starting points. Through these model simulations, we projected future variations of river flow in the Arkansas River and its major tributary of the Canadian River, and attributed river flow variations to four environmental factors, including climate change, cropland change (CC), rising  ${\rm CO_2}$  concentration, and atmospheric nitrogen deposition (Ndep).

While all the 49 simulations started in 1979, our analyses focused on the period of 2000-2099. These simulations can be grouped into five broad categories, i.e., baseline simulations (S0), "Climate-only" simulations (S1), "CConly" simulations (S2), "CO2-only" simulations (S3), "Ndep-only" simulations (S4), and "All-combined" simulations (S5) (Table 1). For the reference simulations (S0), all driving factors were kept constant throughout the simulation period of 2001-2099. Climate conditions were kept at the level of the 20-year average over the period of 1981–2000, while cropland area, CO<sub>2</sub> concentration, and nitrogen deposition were kept at the level in 2000. The fifteen SO reference simulations were to provide a baseline for S1, S2, S3, S4, and S5 simulations to make comparisons. In the fourteen S1 "Climate-only" simulations, climate conditions were the only time-varying driving force in the simulation period of 2001–2099. Contributions of future climate change to river flow were quantified by calculating the difference between S1 simulations and the corresponding SO simulations. Likewise, cropland area, CO<sub>2</sub> concentration, and nitrogen deposition were the only time-varying driving factors in S2, S3, and S4, respectively, while climate conditions in S2, S3, and S4 were kept constant in the simulation period of 2001–2099 using the 20-year average of gridMet climate data in 1981-2000. Contributions of cropland change, rising CO<sub>2</sub> concentration, and nitrogen deposition to river flow were quantified by comparing model results in S2, S3, and S4 with those in the S0.gridMet, respectively. S5 simulations were the "All-combined" simulations, in which all driving factors changed over time. Simulation results in S5 represent DLEM's "best estimate" of future river flow. It is worth noting that future climate data used in this study come from GCMs in the CMIP5 and were not based on the shared socioeconomic pathways in the CMIP6, although we used the same scenario names (i.e., SSP2-RCP45 and SSP5-RCP85) as that in the CMIP6.

## 2.3. Future river flow analyses

We analyzed DLEM-simulated future annual river flow at two levels. For the level-1 analysis, we examined river flow at three watershed outlets, which were (1) the USGS site ID: 07245000, Canadian River near White Field, OK, (2) the USGS site ID: 07194500, Muskogee, OK, and (3) the outlet of the entire Arkansas River Basin. Associated watersheds for the two USGS sites can be found in Fig. S5, representing river hydrological conditions in the ARB's north and south parts, respectively. For the level-2 analysis, we examined river flow in the grids with major river channels (see major river channels in Fig. 1) to illustrate the spatial pattern of river flow changes across the ARB. Next, we calculated the contributions of four environmental factors (climate change, cropland change, rising CO<sub>2</sub> concentration, and atmospheric nitrogen deposition) to river flow changes at the ARB outlet according to the methods described in section 2.2.4. Note that our simulations in this study represent river flow conditions without much human water use and regulation. Therefore, river water diversion and the effects of dams were not considered.

We detected the temporal trend of annual river flow in the ARB over the period of 2000–2099 using the Mann-Kendall (M– K) trend test and the non-parametric Sen's slope estimator (e.g. Ali et al., 2019; Tosunoglu and Kisi, 2017; Yue and Wang, 2004). Next, we analyzed the changed annual river flow in the middle (2040–2059) and at the end (2080–2099) of the 21st century relative to the period from 2000 to 2019.

#### 3. Results

#### 3.1. Comparison and validation

Over the nine years between 2003 and 2011, DLEM-simulated ET was 594.2  $\pm$  48 mm/year, which had a similar magnitude as GLEAM ET (570.4  $\pm$  51.3 mm/year, Fig. 3). MTE and MODIS had a relatively lower ET rate (531  $\pm$  31.3 mm/year and 427.9  $\pm$  54.2 mm/year, respectively). According to Velpuri et al. (2013), MODIS underestimated ET in cropland, grassland, and shrubland by 8–14 % compared to AmeriFlux measurements, which partially explained the lower MODIS ET than the other three datasets in the central and western ARB. All four datasets simulated a declining ET spatial pattern from east to west.

Interannual ET variation in the four datasets was similar to each other (Fig. S6). During 2003–2011, the four datasets showed that 2011 was the year with the lowest ET, which were 19.1 %, 27.5 %, 19.9 %, and 13.3 % lower than the 9-year average ET for DLEM, MODIS, GLEAM, and MTE, respectively. Meanwhile, the four datasets showed that 2007 was the year with the highest ET, which were 8.2 %, 15.8 %, 9.8 %, and 6.1 % higher than the 9-year average for DLEM, MODIS, GLEAM, and MTE, respectively. Additionally, all four datasets showed annual ET in the ARB had a significant declining trend over the nine years with declining rates of – 8.5 mm/year, – 6.2 mm/year, – 5.9 mm/year, and – 4.0 mm/year for DLEM, MODIS, GLEAM, and MTE, respectively.

The DLEM-simulated monthly river flow was validated against measurements at USGS gauge stations (Fig. 4). NSE of DLEM simulations reached 0.66, 0.65, 0.68, 0.54, and 0.59 at the five stations of site 07,191,500 (Chouteau, OK), site 07,194,500 (Muskogee, OK), site 07,263,450 (Murray Dam, AR), site 07,245,000 (Canadian River near White Field, OK), and site 07,249,455 (Fort Smith, AR). NSE results indicated that DLEM captured the temporal variation of river flow in the ARB. However, PBIAS was negative at four sites (-12.6 % at site 07194500, – 8.3 % at site 07263450, –23.3 % at site 07245000, and – 8.8 % at site 07249455) and positive at one site (15.4 % at site 07191500). PBIAS results indicated the magnitude of DLEM-simulated river flow was generally consistent with USGS measurements, but with a tendency to overestimate the ARB river flow. This was likely caused by the diversion of Arkansas River water for cropland irrigation and public supply, which was not considered in our simulations.

## 3.2. Future changes in environmental conditions

According to the bias-corrected climate data simulated by seven GCMs in CMIP5, temperature in the ARB will increase significantly in both the RCP45 and the RCP85 scenarios throughout the 21st century (Fig. 5). Temperature will increase by 1.6  $\pm$  0.29 °C and 2.2  $\pm$  0.44 °C from the period of 2000–2019 to the period of 2040–2059 in the RCP45 and RCP85 scenarios, respectively (Table 2 and S1). Between the first and last 20-year periods in the 21st century, temperature will increase by 2.1  $\pm$  0.48 °C and 4.7  $\pm$  0.67 °C in the RCP45 and the RCP85 scenarios, respectively. The increasing trend in future temperature is relatively consistent between all the seven GCMs (Fig. S7).

Precipitation will have a different pattern of change to temperature. The model-ensemble mean results showed that average precipitation in 2040–2059 and 2080–2099 would be lower than that in 2000–2019 (Table 2). Compared to the period of 2000–2019, precipitation in

2040–2059 will decrease by 28  $\pm$  32.9 mm/year (3.8 %) and 28.3  $\pm$  48.8 mm/year (3.8 %) in the RCP45 and the RCP85, respectively. Compared to the period of 2000–2019, precipitation in 2080–2099 will decrease by 13.1  $\pm$  31.7 mm/year (1.8 %) and 32.7  $\pm$  39.3 mm/year (4.4 %) in the RCP45 and the RCP85, respectively (Table S1). It is worth noting that the changes in regional precipitation are associated with considerable variations between GCMs (Fig. S7). For example, in the RCP85, the range of precipitation change between the period of 2080–2099 and the period of 2000–2019 is from – 107.7 mm/year

#### 3.3. Future evapotranspiration

For the ARB as a whole, the changing trend in regional ET will be insignificant during 2000–2099 (p-value > 0.05, M– K trend test) in both the SSP2-RCP45 and the SSP5-RCP85 (Fig. S10). In the SSP2- RCP45 scenario, ET in the ARB was  $608.7 \pm 9.3$  mm/year in 2000-2019 and will be  $601.8 \pm 16.3$  mm/year in 2040-2059 and  $611 \pm 13.2$  mm/year in 2080-2099 (Table 3). In the SSP5-RCP85 scenario, ET in the ARB was  $605.9 \pm 14$  mm/year in 2000-2019 and

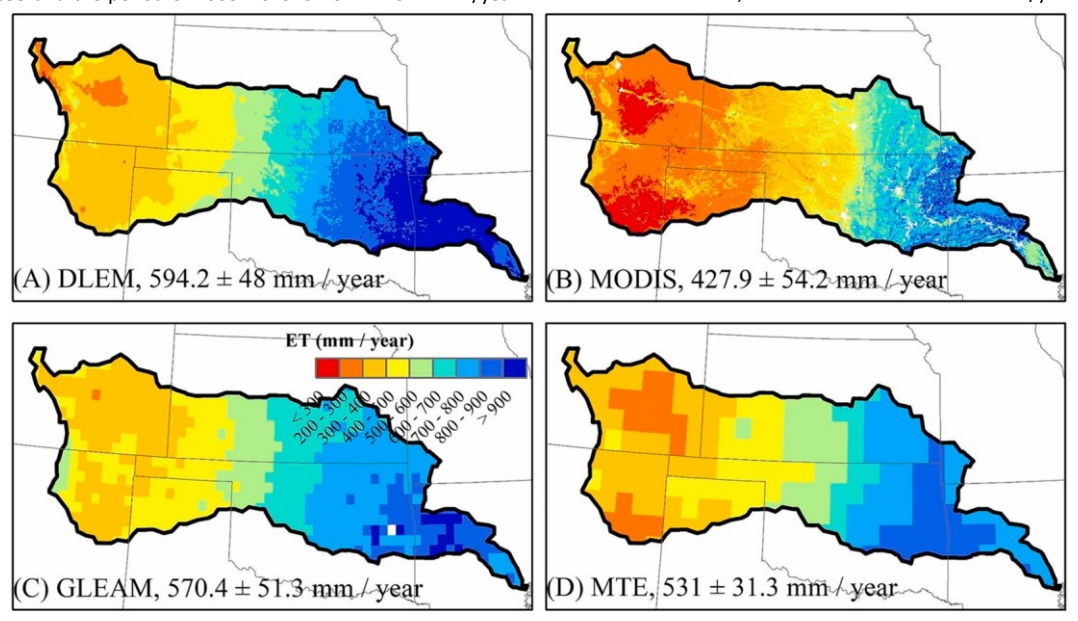


Fig. 3. Spatial pattern of annual evapotranspiration (mm/year) during 2003–2011 from DLEM (A), MODIS (B), GLEAM (C), and MTE (D).

(IPSL-CM5A-LR) to 37 mm/year (CCSM4), indicating the necessity to include multiple GCMs and report the uncertainty range when projecting future river flow. Regarding the spatial pattern, precipitation reduction will occur over most of the ARB (Fig. S8). Compared to the period of 2000–2019, the reduced precipitation in 2040–2059 will take place in 99.9 % of the ARB in the RCP45 and 98.1 % of the ARB in the RCP85. The reduced precipitation in 2080–2099 will take place in 90.6 % of the ARB in the RCP45 and 91.9 % of the ARB in the RCP85. Precipitation will show a more significant reduction in the southern ARB than the northern ARB under both scenarios, and the increased precipitation will be primarily in eastern Kansas.

The temporal variations of cropland area in the ARB will differ between the SSP2-RCP45 and the SSP5-RCP85. In the SSP2-RCP45, the cropland area will increase from 86,631 km<sup>2</sup> in 2000–2019 to 104,765 km<sup>2</sup> in 2040–2059 (Table 2). Cropland expansion in this period will primarily happen in the grassland areas (Fig. S9). The cropland area will further increase to 123,356 km<sup>2</sup> in 2080–2099. However, cropland expansion in this period will be primarily in eastern Oklahoma and Kansas forest areas. In the SSP5-RCP85, the cropland area will be at a relatively stable level of ~ 82,156 km<sup>2</sup> over the entire study period. CO<sub>2</sub> concentration will increase continuously at different increasing rates in the RCP45 and the RCP85 (Fig. 4). The average CO<sub>2</sub> concentration was 388 ppm from 2000 to 2019. In the RCP45, the average CO2 concentration will increase to 486 ppm in 2040–2059 and 535 ppm in 2080–2099. Compared to the RCP45, CO<sub>2</sub> concentration in the RCP85 will increase at a faster rate and reach 535 ppm in 2040-2059 and 837 ppm in 2080-2099. Atmospheric nitrogen deposition rates in the future will be lower compared to the contemporary period in both the SSP2- RCP45 and the SSP5-RCP85 (Fig. 4). Nitrogen deposition in the period of 2000–2019 was 0.88 g  $N/m^2/year$ . In the RCP45, the average nitrogen deposition rates will decrease to 0.61 g N/m<sup>2</sup>/year in 2040-2059 and 0.46 g N/m<sup>2</sup>/year in 2080–2099. In the RCP85, the average nitrogen deposition rates will decrease to  $^{\sim}$  0.7 g N /  $m^2$  / year in the 2030 s and be a relatively stable level thereafter. The decline in future nitrogen deposition is consistent with the trend over recent two decades as a result of the Clean Air Act and other ruls constraining industrial nitrogen gas emissions (Gilliam et al., 2019).

will be 601.8 ± 31.5 mm/year in 2040–2059 and 609.6 ± 16.1 mm/year in 2080–2099. It is apparent that the eastern and western ARB (with the 98th meridian as the dividing line, i.e., the dotted red line in Fig. 6) have contrasting patterns of ET change (Table 3). In the eastern ARB, ET in the SSP2-RCP45 scenario will increase by 5.9 mm/year during 2040–2059 and 13.3 mm/year during 2080–2099 compared to the period of 2000–2019. ET in the SSP5-RCP85 scenario will increase by 9.1 mm/year during 2040–2059 and 25.9 mm/year during 2080–2099 compared to the period of 2000–2019. On the contrary, in the western ARB, ET in the SSP2-RCP45 scenario will decrease by 14.7 mm/year during 2040–2059 and 4.5 mm/year during 2080–2099 compared to the period of 2000–2019. ET in the SSP5-RCP85 scenario will decrease by 12.3 mm/year during 2040–2059 and 10.2 mm/year during 2080–2099 compared to the period of 2000–2019.

The eastern ARB is a relatively humid region with an Aridity Index of 0.8, while the western ARB is a relatively dry region with an Aridity Index of 0.32 (Fig. S3). We developed a spatial map of Pearson's correlation coefficient between the interannual variations in the DLEM- simulated ET and annual precipitation (Fig. S11). This map shows an increasing trend in the precipitation-ET correlation from east to west, indicating a stronger precipitation impact on ET in the western ARB than that in the eastern ARB. According to the Budyko curve that describes the geographic difference in annual evapotranspiration in relation to the abundance of annual precipitation and radiation (Budyko, 1951), ET is limited by water supply in the dry area and by radiation in the humid zone. Despite the reduced future precipitation over most of the ARB, the eastern ARB will have an increased ET because of the higher evaporative water demand in the atmosphere caused by climate warming. In the western ARB, ET will decrease along with the reduced precipitation and limited water supply. The different patterns of ET change between the eastern ARB and the western ARB will negate each other, resulting in an insignificant ET change in the 21st century when considering the entire

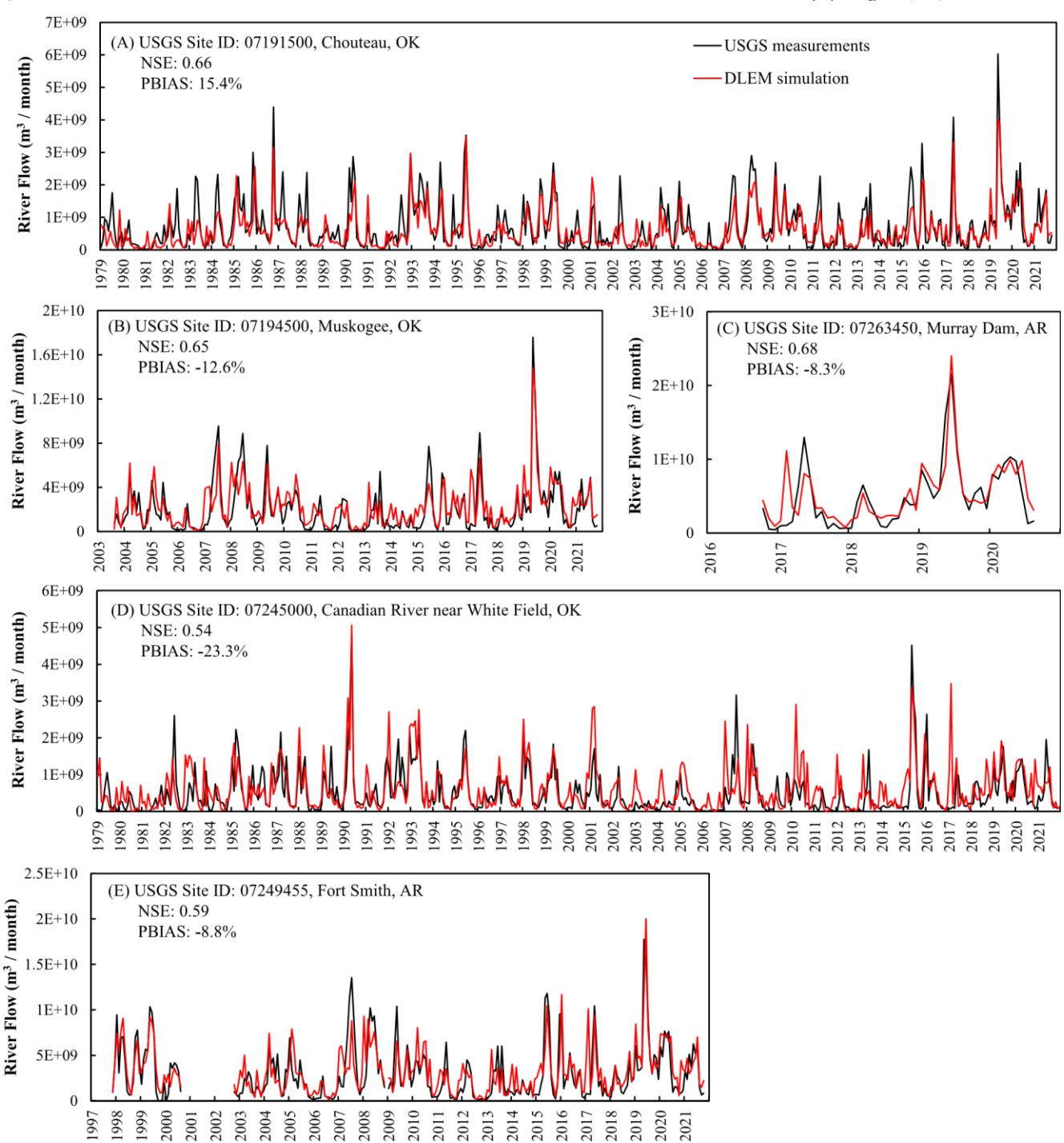


Fig. 4. Comparison of DLEM-simulated monthly river flow against USGS measurements at five gauge stations in the Arkansas River Basin. (A) Site ID: 07191500, Chouteau, OK, (B) site ID: 07194500, Muskogee, OK, (C) site ID: 07263450, Murray Dam, AR, (D) site ID: 07245000, Canadian River near White Field, OK, and (E) site ID: 07249455, Fort Smith, AR. Abbreviations: NSE: Nash-Sutcliffe Efficiency; PBIAS: percent bias.

ARB.

north of the ARB (Fig. S5), respectively. For the Canadian River – White Field.

## 3.4. Future river flow

M– K trend test showed that annual river flow from 2000 to 2099 will have significant decreasing trends (p-value less than 0.05) in both the SSP2-RCP45 and the SSP5-RCP85 at the three locations of (1) the USGS site ID: 07245000, Canadian River near White Field, OK, (2) the USGS site ID: 07194500, Muskogee, OK, and (3) the outlet of the entire ARB (Fig. 7). We used the USGS site on the Canadian River — White Field and the USGS site on the Arkansas River — Muskogee to represent river hydrological conditions in the south and

north of the ARB (Fig. S5), respectively. For the Canadian River – White Field, changing rates of annual river flow (i.e., Sen's slope) will be –  $1.6 \times 10^7 \, \text{m}^3$ /year in the SSP2-RCP45 and –  $3.6 \times 10^7 \, \text{m}^3$ /year in the SSP5-RCP85. For the Arkansas River - Muskogee, changing rates of annual river flow will be

 $-4.8 \times 10^7$  m³/year in the SSP2-RCP45 and  $-1.1 \times 10^8$  m³/year in the SSP5-RCP85. At the outlet of the entire ARB, changing rates of annual river flow will be  $-8.5 \times 10^7$  m³/year in the SSP2-RCP45 and  $-1.9 \times 10^8$  m³/year in the SSP5-RCP85. The declining rate of annual river flow

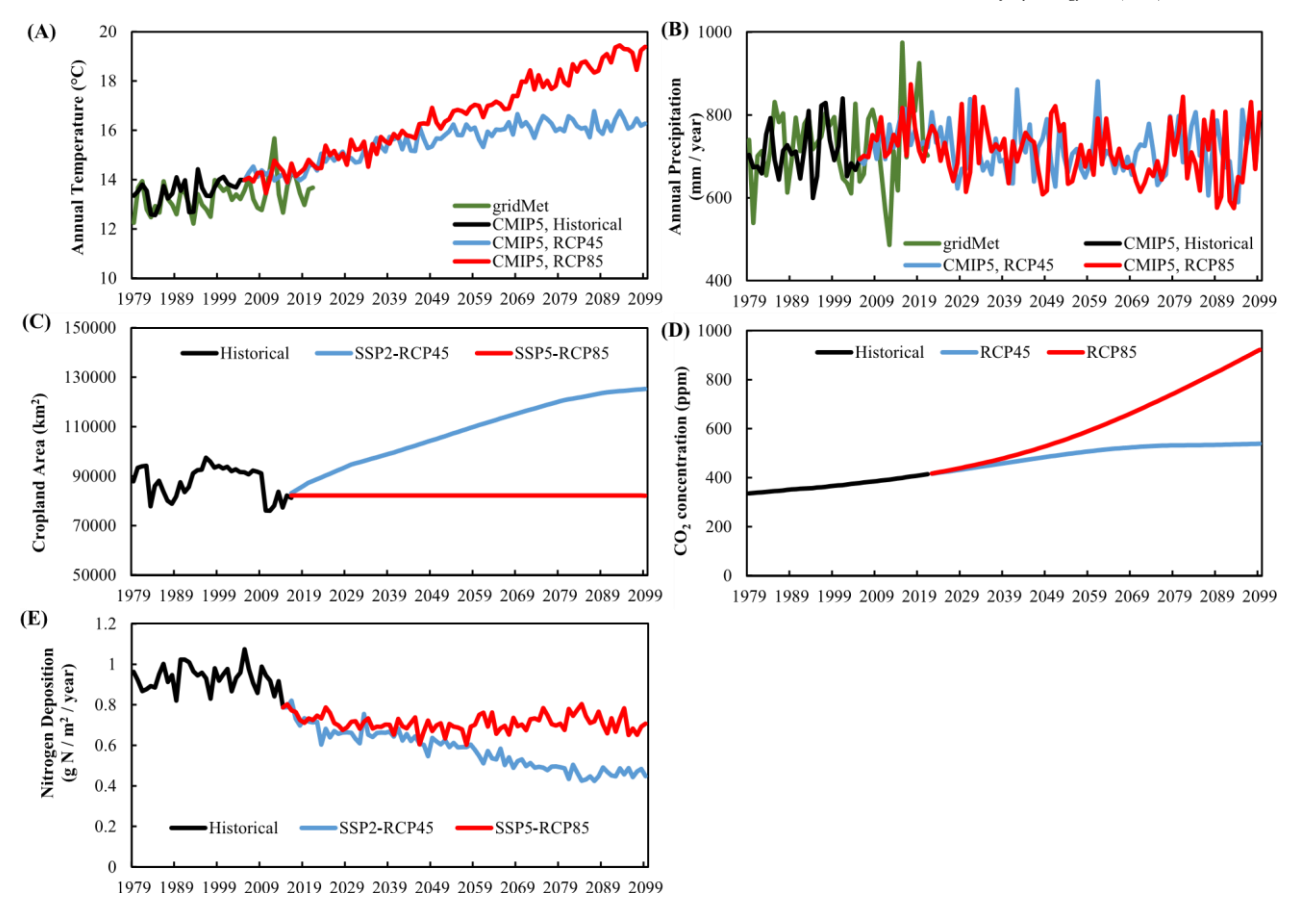


Fig. 5. Interannual variations of environmental factors in the Arkansas River Basin in the historical and future periods. (a) Annual temperature, (b) annual precipitation, (c) cropland area, (d) CO<sub>2</sub> concentration, and (e) annual rate of atmospheric nitrogen deposition.

Table 2 Statistics of environmental factors (annual temperature, precipitation, cropland area,  $CO_2$  concentration, and nitrogen deposition) in the periods of 2000–2019, 2040–2059, and 2080–2099.

	2000–2019	2040-2059	2080-2099
Annual Temperature (°C) RCP45	•		
	14.1 ± 0.26	15.7 ± 0.49	16.2 ± 0.48
RCP85	14.1 ± 0.2	$16.3 \pm 0.64$	18.8 ± 0.85
Annual Precipitation (mm/year)			
RCP45	733.8 ± 22.2	705.8 ± 38.5	720.7 ± 38.5
RCP85	735.6 ± 18.6	707.3 ± 45.7	702.9 ± 32.6
Cropland Area (km²)			
SSP2-RCP45	86,631	104,765	123,356
SSP5-RCP85	86,134	82,157	82,156
CO <sub>2</sub> Concentration (ppm) RCP45			
	388	486	535
RCP85	388	535	837
Nitrogen Deposition (g N/m²/ year)			
SSP2-RCP45	0.88	0.61	0.46
SSP5-RCP85	0.88	0.68	0.72

in the SSP5-RCP85 scenario will be  $2.2 \approx 2.3$  times the declining rate in the SSP2-RCP45 scenario at the three locations.

From the first 20 years to the last 20 years of the 21st century, river flow in the SSP2-RCP45 will decrease by 13.4 %, 11.4 %, and 12.1 % at the three locations of the Canadian River – White Field, the the Arkansas River – Muskogee, and the ARB outlet, respectively, while river flow in the SSP5-RCP85 will decrease by 33.7 %, 27.3 %, and 27.9 % at the three locations, respectively (Table 4). River flow in the Canadian River watershed will have a larger percentage reduction than that in the northern ARB. Notably, the reduced river flow in the SSP2-RCP45 scenario will take place from the beginning to the middle of the 21st century, while the reduced river flow in the SSP5-RCP85 scenario will happen throughout the entire 21st century.

The shaded area and box plots in Fig. 7 indicate the general consistency in the decreasing trend of the simulated river flow driven by climate data from 7 GCMs. For example, at the ARB outlet in the SSP2- RCP45, simulations driven by 6 climate datasets show declined river flow in the middle of the 21st century and simulations driven by 5 climate datasets show declined river flow by the end of the 21st century. Additionally, in the SSP5-RCP85, simulations driven by 6 climate datasets show declined river flow in the middle of the 21st century and simulations driven by all 7 climate datasets show declined river flow by the end of the 21st century. This result consolidates the general declining trend in the ARB river flow despite the variations in future climate conditions projected by different GCMs.

The percentage reduction of river flow will show considerable variations over different areas in the ARB (Fig. 8). In the SSP2-RCP45 during 2040–2059, the greatest percentage reduction (over 20 %) will happen in the southwestern ARB, i.e., the North Canadian River, the Canadian River, and the Cimarron River to the west of the 99th meridian. Other areas of the ARB will have a reduction in river flow between 10 % and 20 % (Fig. 8A). In the SSP2-RCP45 during 2080 – 2099, the southwestern ARB (i.e., the North Canadian River, the Canadian River, and the Cimarron River to the west of the 99th meridian) will also show the largest percentage reduction of over 20 % in river flow. The Arkansas River to the west of the 97th meridian will have a reduction of 15–20 %, while other areas of the ARB will have a relatively smaller percentage reduction of 10–15 % (Fig. 8B). In the SSP5-RCP85 during 2040–2059, the largest percentage reduction (over 20 %) will happen in the southwestern ARB along the Canadian River and the North Canadian River.

Table 3
Statistics of the simulated evapotranspiration (ET, mm/year) in the entire ARB, the western ARB, and the eastern ARB in the three 20-year periods of 2000–2019, 2040–2059, and 2080–2099

	ET in 2000–2019	ET in 2040–2059	ET in 2080–2099	ET change	es between 2040 and 2059 and 2000–2019	ET changes between 2080 and 2099 and 2000– 2019
ARB						
SSP2-RCP45	608.7 ± 9.3	601.8 ± 16.3	611.0 ± 13.2	- 6.8		2.3
SSP5-RCP85	605.9 ± 14.0	601.8 ± 31.5	609.6 ± 16.1	- 4.1		3.6
Western						
ARB						
SSP2-RCP45	457.6 ± 12.0	442.9 ± 19.4	453.1 ± 23.5	- 14.7		- 4.5
SSP5-RCP85	455.1 ± 12.1	442.8 ± 29.6	444.9 ± 17.9	- 12.3		- 10.2
Eastern ARB						
SSP2-RCP45	851.4 ± 21.5	857.3 ± 18.4	864.7 ± 11.9	5.9		13.3
SSP5-RCP85	848.2 ± 19.0	857.3 ± 39.3	874.1 ± 26.1	9.1		25.9
(A) SSP2-	RCP45, ET <sub>204</sub>	10 - 2059 ET 2000 -	2019 ET Difference (m	nm / year)	(B) SSP2-RCP45, ET <sub>2080 - 209</sub>	99 - ET <sub>2000 - 2019</sub>
				\$ \$ \$ \$ \$		

Fig. 6. Spatial patterns of the changed evapotranspiration (ET) over three 20-year periods of 2000–2019, 2040–2099, and 2080–2099 in the SSP2-RCP45 and the SSP5-RCP85. (A) ET difference between the period of 2040–2059 and the period of 2000–2019 in the SSP2-RCP45, (B) ET difference between the period of 2080–2099 and the period of 2000–2019 in the SSP2-RCP45, (C) ET difference between the period of 2040–2059 and the period of 2000–2019 in the SSP5-RCP85, and (D) ET difference between the period of 2080–2099 and the period of 2000–2019 in the SSP5-RCP85. The red dash line represents the 98th meridian.

The percentage reduction of river flow in the Arkansas River will be between 15 % and 20 % (Fig. 8C). In the SSP5-RCP85 during 2080–2099, river channels to the west of the 95th meridian, including the Arkansas River, the North Canadian River, the Canadian River, and the Cimarron River, will have a considerable river flow reduction of over 30 %. The Neosho River will have a decrease of 20–25 % and the Arkansas River to the east of the 95th meridian will have a reduction of 25–30 % (Fig. 8D). Overall, river flow in all river channels of the ARB will decline in the 21st century with the most significant reduction in the western, particularly the southwestern ARB.

## 3.5. Contributions of environmental factors

(C) SSP5-RCP85, ET<sub>2040 - 2059</sub> - ET<sub>2000 - 2019</sub>

By calculating differences between the 49 model simulations (Table 1), we quantified the contributions of four environmental factors (climate change, cropland change, rising  $CO_2$  concentration, and atmospheric nitrogen deposition) to the changed river flow at the ARB outlet (Fig. 9). Percentage contribution (%) of a specific environmental factor was computed as the ratio of its impact on river flow change to the combined effect of the four timevarying environmental factors. It is noteworthy that the sum of percentage contributions from the four environmental factors does not equal 100 %

because the interactions between environmental factors will make contributions to the changed river flow but are not presented here.

(D) SSP5-RCP85, ET<sub>2080 - 2099</sub> - ET<sub>2000 - 2019</sub>

In both the SSP2-RCP45 and the SSP5-RCP85 scenarios, climate warming and drying were identified as the primary environmental factors for the decreased river flow. Contributions of climate change to the decreased river flow in the SSP2-RCP45 will be 85.3 % during 2040–2059 and 95.3 % during 2080–2099. Contributions of climate change to the decreased river flow in the SSP5-RCP85 will be 80.6 % during 2040–2059 and 77.1 % during 2080–2099.

Cropland area in the ARB will increase continuously in the SSP2- RCP45 but keep at a relatively stable level in the SSP5-RCP85. In the SSP2-RCP45, cropland change will decrease river flow in the first half of the 21st century, contributing 5.1 % to the reduced river flow in 2040–2059. However, the effect of cropland change will reverse in the second half of the 21st century. During the period 2080–2099, cropland change will increase the river flow of the Arkansas River, contributing

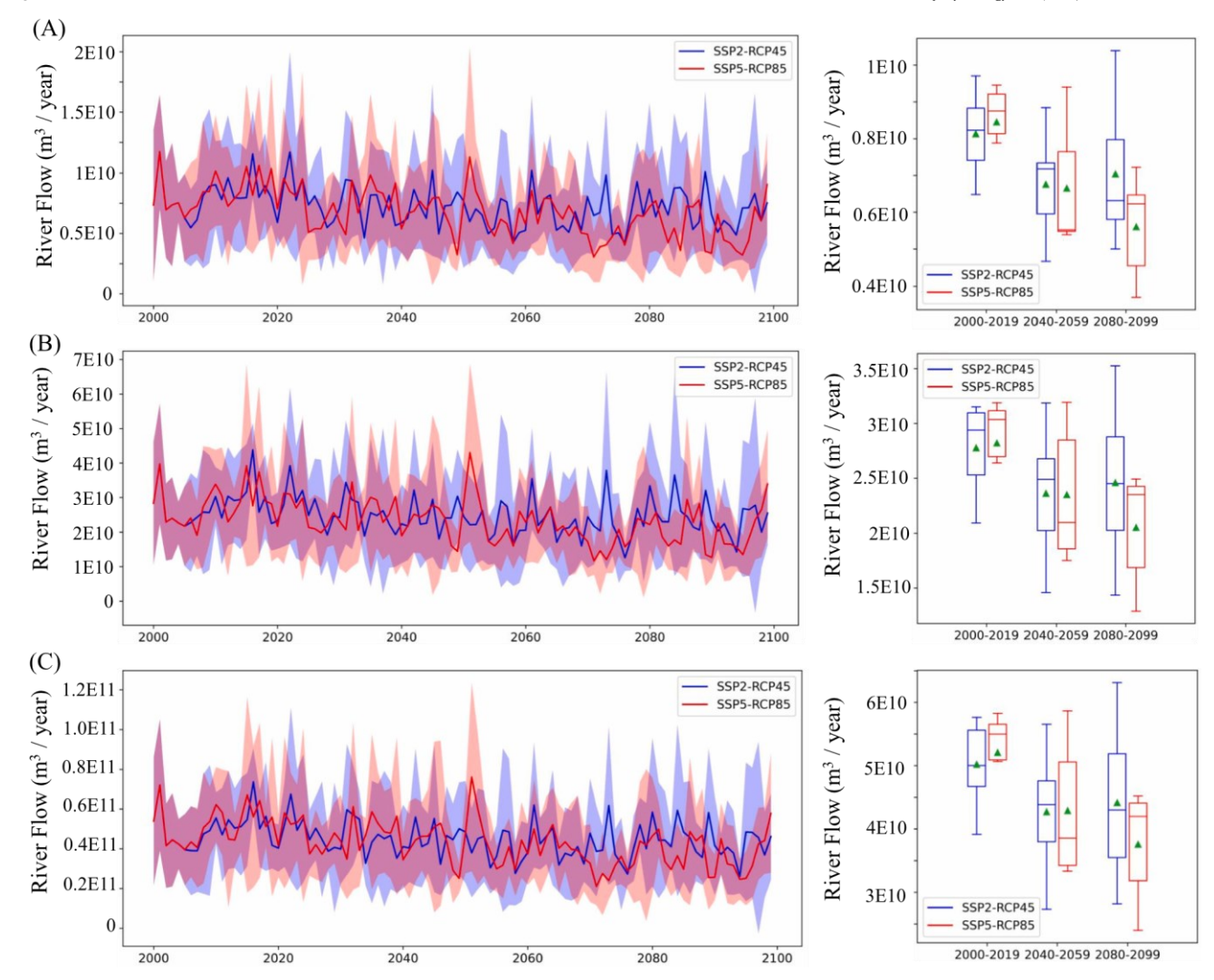


Fig. 7. Annual river flow from 2000 to 2099 in the SSP2-RCP45 and the SSP5-RCP85 scenarios at the three locations of (A) the USGS site ID: 07245000, Canadian River near White Field, OK, (B) the USGS site ID: 07194500, Muskogee, OK, and (C) the outlet of the entire Arkansas River Basin. The pink and blue shaded areas are the standard deviations of the simulated river flow driven by seven sets of climate data in the SSP2-RCP45 and the SSP5-RCP85 scenarios, respectively. Box plots in the right column show average river flow in the three periods of 2000–2019, 2040–2049, and 2080–2099. Green triangles in the box plots are the average of the simulated river flow driven by seven sets of climate data.

Table 4
Model-simulated river flow (m³/year) at three locations in the Arkansas River Basin over three 20-year periods of the 21st century and under two climate and socioeconomic scenarios.

	SSP2-RCP45			SSP5-RCP85		
	2000–2019	2040–2059	2080–2099	2000–2019	2040–2059	2080–2099
Canadian River – White Field	8.1 × 10 <sup>9</sup>	6.8 × 10 <sup>9</sup>	7.0 × 10 <sup>9</sup>	8.5 × 10 <sup>9</sup>	6.7 × 10 <sup>9</sup>	5.6 × 10 <sup>9</sup>
Arkansas River – Muskogee	$2.8 \times 10^{10}$	$2.4 \times 10^{10}$	$2.5 \times 10^{10}$	$2.8 \times 10^{10}$	$2.4 \times 10^{10}$	$2.1 \times 10^{10}$
ARB outlet	5.0 × 10 <sup>10</sup>	$4.3 \times 10^{10}$	$4.4 \times 10^{10}$	5.2 × 10 <sup>10</sup>	$4.3 \times 10^{10}$	3.8 × 10 <sub>10</sub>

-17.6% to the overall declining river flow pattern. In the SSP5-RCP85, cropland change will have a negligible effect and the contributions of cropland change will be 3.8 % in 2040–2099 and 2.2 % in 2080–2099.

The rising CO<sub>2</sub> concentration will affect ecosystem hydrological processes by altering leaf stomatal conductance, stomatal density, and vegetation foliage area (Gedney et al., 2006; Liu et al., 2018; Piao et al., 2007; Tao et al., 2014). Our results showed that the rising CO<sub>2</sub> concentrations would reduce river flow in the ARB. In the SSP2-RCP45, the rising CO<sub>2</sub> will contribute 11.8 % of the decreased river flow in 2040–2099 and 24.9 % of the reduced river flow in 2080–2099. In the SSP5-RCP85, the rising CO<sub>2</sub> will contribute 11.7 % of the reduced river flow in 2040–2099 and 13.6 % of the decreased river flow in 2080–2099.

Atmospheric nitrogen deposition can modulate ecosystem evapotranspiration by affecting vegetation conditions (Dickinson et al., 2002;

Mao et al., 2015; Shi et al., 2013). In this study, we found the changes in future nitrogen deposition will have a relatively minor effect compared to the other three factors. The reduced nitrogen deposition will result in lower ecosystem evapotranspiration and then, increased river flow. In the SSP2-RCP45, contributions of the reduced nitrogen deposition to the decreased river flow will be  $-2.2\,\%$  in 2040–2099 and  $-6.4\,\%$  in 2080–2099. In the SSP5-RCP85, contributions of the reduced nitrogen

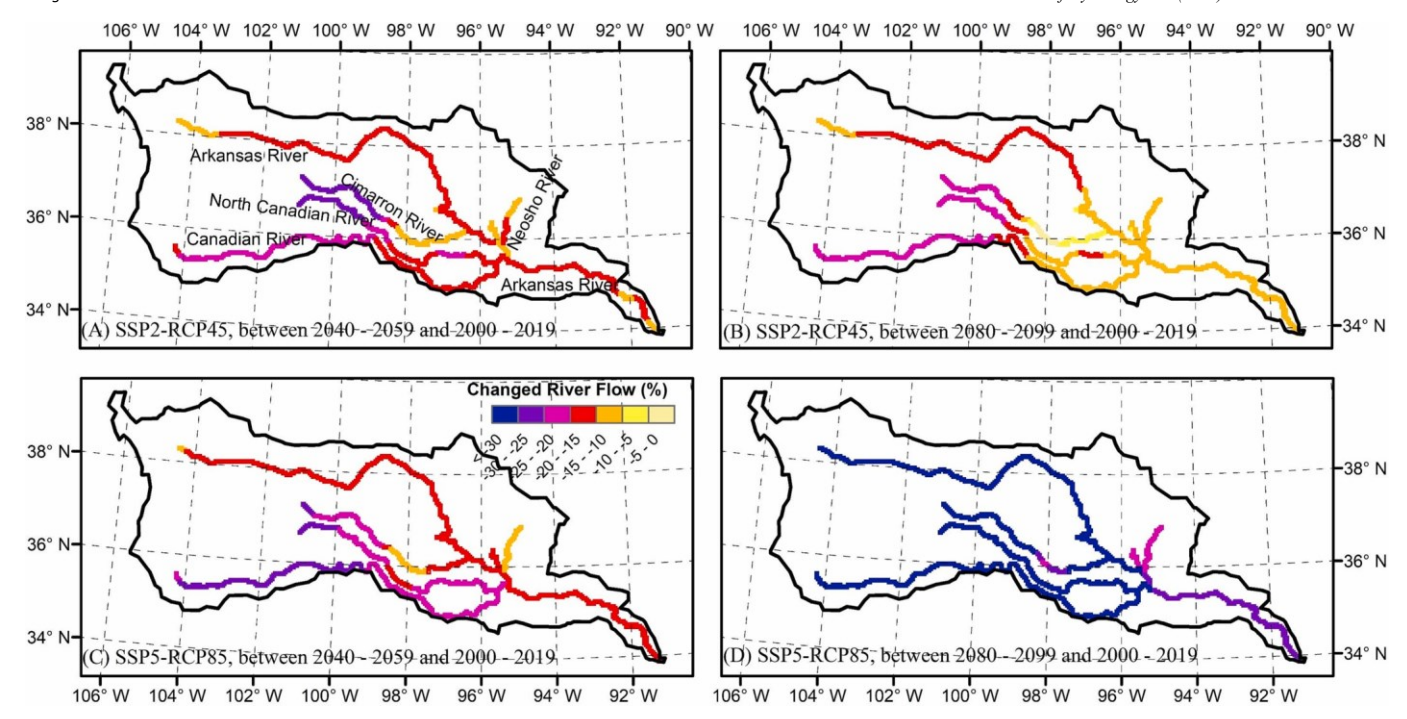


Fig. 8. Percentage changes of river flow in the major river channels between the periods of 2040–2059 and 2000–2019 in the SSP2-RCP45 scenario (A), between the periods of 2080–2099 and 2000–2019 in the SSP2-RCP45 scenario (B), between the periods of 2040–2059 and 2000–2019 in the SSP5-RCP85 scenario (C), and between the periods of 2080–2099 and 2000–2019 in the SSP5-RCP85 scenario (D). Polylines of river channels were thickened for better visualization.

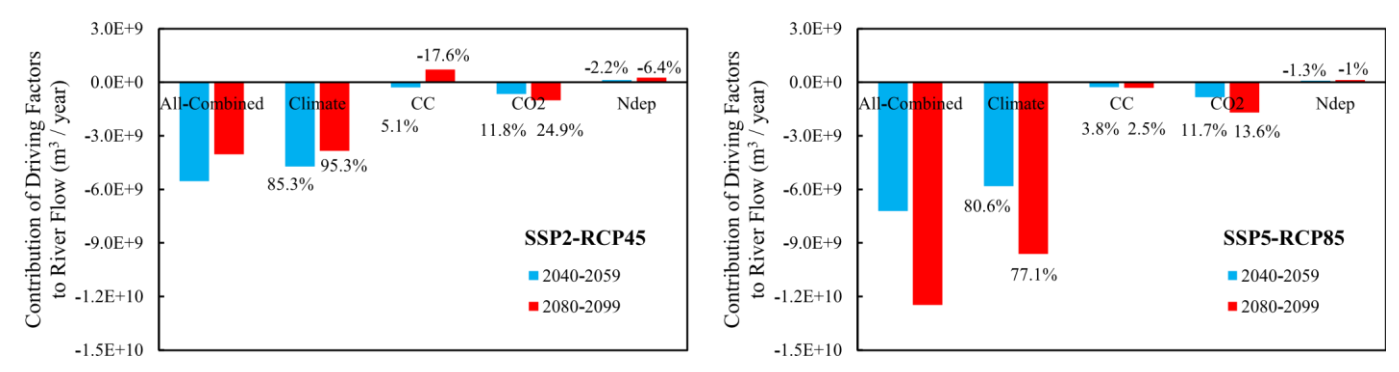


Fig. 9. Contributions of climate change, cropland change (CC), rising  $CO_2$  concentration, and atmospheric nitrogen deposition (Ndep) to the changed river flow at the outlet of the entire Arkansas River Basin. Blue bars show river flow differences between the period of 2040–2059 and the period of 2000–2019. Red bars show river flow differences between the period of 2090–2099 and the period of 2000–2019. The left and right panels show the results in the SSP2-RCP45 and in the SSP5- RCP85, respectively. Percentages above/below the bars are the contributions of environmental factors to the overall river flow changes.

deposition to the decreased river flow will be – 1.3 % in 2040–2099 and – 1% in 2080–2099.

## 4. Discussion

## 4.1. Mechanisms controlling Long-term river flow

The long-term changes of river flow at the decadal scale largely depend on the balance between precipitation and ecosystem ET (Piao et al., 2007). Variation in precipitation has a direct impact through changing soil moisture and runoff generation. Our results identified the widespread reduction in precipitation as one major factor for the decreased river flow in the middle and at the end of the 21st century under both the RCP45 and RCP85 scenarios (Section 3.5). Nevertheless, future changes in ecosystem ET will have a more complex pattern because it can be modulated by weather conditions, soil properties, vegetation type, and ecosystem physiological and structural characteristics (Mao et al., 2015; Piao et al., 2007).

The ARB has a large span of aridity in the east—west direction. Our model simulated contrasting patterns of ET changes between the western ARB and the eastern ARB in the context of future climate warming and drying (section 3.3). Climate warming will cause increases in atmospheric water demand and

ecosystem potential ET (Scheff and Frierson, 2014). In the arid western ARB, the increased atmospheric water demand will not lead to higher actual ET because of the limited water supply under the impacts of reduced precipitation. This result is consistent with the declining ET in global semiarid regions over recent decades caused by the limited moisture supply (Jung et al., 2010; Yang et al., 2019b). On the contrary, the humid eastern ARB will have an increased actual ET because of the increased atmospheric water demand and sufficient water supply. This contrasting ET changing pattern can be well explained by Budyko's framework, which describes the dependence of evapotranspiration on water and energy availability (Li et al., 2013).

CO<sub>2</sub> impacts on evapotranspiration and river flow have not been fully understood. C3 and C4 plants have different photosynthesis processes (Calvin Cycle vs Hatch and Slack Cycle) and are different in their response to the increased CO<sub>2</sub> concentration. Large-scale free-air CO<sub>2</sub> enrichment (FACE) experiments showed that leaf stomatal conductance decreased with the rising CO<sub>2</sub> concentration for C3 species, but showed little responses for C4 species (Ainsworth and Long, 2005; Ainsworth and Rogers, 2007). Some studies attributed a considerable part of the increased global river flow in the 20th century to CO<sub>2</sub>-induced reduction in stomatal conductance (Gedney et al., 2006), while other studies indicated that the rising CO<sub>2</sub> had a limited effect on river flow because CO<sub>2</sub> can act as a plant fertilizer to increase foliage area and

increase plant transpiration (Piao et al., 2007). The ARB and the southern Great Plains have a large fraction of C4 grasses (Still et al., 2003), which make stomatal conductance less sensitive to the rising  $CO_2$  compared to C3 grasses and forests. In our simulations, future rising  $CO_2$  will increase ET and decrease river flow in the ARB because the positive  $CO_2$  effect on ET through enhancing foliage area will outweigh its negative effect on ET through reducing stomatal conductance.

Impacts of land-use change on river flow have been investigated over many basins across the globe. The general conclusion is that land conversion from forests to croplands and pastures leads to increased river flow (e.g. Schilling et al., 2010; Siriwardena et al., 2006; Tao et al., 2014; Zhang and Schilling, 2006). Our analysis on the LUH2 land-use data (Hurtt et al., 2020) showed that cropland area in the ARB will increase in the SSP2-RCP45 scenario but keep at a relatively stable level in the SSP5-RCP85 scenario. In the SSP2 scenario, global demand for crop and livestock products increases moderately (Popp et al., 2017), leading to the increased cropland area in the ARB. In the first half of the 21st century, cropland expansion in the ARB will primarily happen in the grassland area. As grassland and cropland have a similar ET magnitude (Yue et al., 2022), our results showed that the replacement of grasslands by croplands will have a small impact on river flow. However, land conversion from forests to croplands after the 2050 s will lead to increased surface runoff and river flow. Land-use pattern in the SSP5 scenario is characterized by moderate tropical deforestation but little changes in North America because agricultural products are not necessarily produced domestically in the globalized world (Krause et al., 2019; Popp et al., 2017). Therefore, our simulation showed a minor effect of cropland change on river flow in the SSP5-RCP85 scenario.

## 4.2. Implications for water management

Agricultural irrigation and public supply consumed a large portion of surface water in the ARB. The demand for water resources is expected to increase during the 21st century given the continued trends in climate warming and population growth (Vor" osmarty et al., 2000; Ward and "Pulido-Velazquez, 2008). However, the ARB is projected to have less river flow and reduced surface water availability, particularly in the western and southwestern ARB (section 3.4), which requires the implementation of effective water management and conservation strategies to meet the growing water demand. To maintain long-term water resource sustainability, it is essential to improve the efficiency and productivity of agricultural irrigation systems (Evett et al., 2020) and apply more conservative indoor and outdoor water use strategies (Maggioni, 2015).

A significant amount (~30 %) of surface water withdrawals have been used for irrigation in the ARB (Tortorelli, 2009). Thus, the improvement in irrigation efficiency is a potential strategy to adapt to the reduced river flow. In 2018, over 85 % of the irrigated area in the Southern High Plains used the centerpivot sprinkler irrigation system. In Kansas, the irrigated land area with a center-pivot sprinkler irrigation system increased from 50 % to 92 % during 1990–2012 (Evett et al., 2020; Rogers and Lamm, 2008). This irrigation system has greatly improved water use efficiency compared to the traditional gravity irrigation system (Levidow et al., 2014). To further improve irrigation efficiency, it could be necessary to adopt more efficient irrigation strategies (such as the subsurface drip irrigation system (Lamm et al., 2012)), more accurate irrigation scheduling (Gu et al., 2020), and precision irrigation systems to place water where it can be effectively used by crops (Evett et al., 2020). Additionally, genetic modification is being widely studied to develop new crop cultivars with improved drought tolerance but without yield penalty (Khan et al., 2019). In the future, planting drought-tolerant crop cultivars could be a helpful strategy to reduce irrigation water use and maintain agricultural sustainability in the

Conservative household water use strategies could be of particular importance for cities in the Canadian River Basin, such as the Oklahoma City metropolitan area, which will experience more severe river flow reduction than the other watersheds. For household water use, the current drought-related prescriptive policies and price-based water conservation strategies (Wichman et al., 2016) may become the norm in the future. Since outdoor water uses are

more elastic (Mansur and Olmstead, 2012), the prescriptive policy limiting outdoor irrigation can be effective in reducing the household level of water use (Maggioni, 2015). Additionally, price-based regulation and water conservation incentives can be effective for urban water conservation (Lee et al., 2013; Olmstead and Stavins, 2009). Low-income households could be more sensitive to price and incentive conservation strategies, while prescriptive policies have uniform responses across all household income levels (Wichman et al., 2016).

#### 4.3. Uncertainties and future needs

We used DLEM to simulate ARB river flow dynamics in the 21st century driven by a series of environmental factors. Future climate data is one of the major uncertainty sources in this study. It is known that GCMs produced divergent future climate patterns, which come from the incomplete representation of regional-scale processes, inadequate parameterization skills, imperfect initial conditions, and relatively coarse resolution (Almazroui et al., 2021). Thus, we included future climate data simulated by seven GCMs in the CMIP5 project to drive DLEM and reported the standard deviation to document the uncertainty in the projected river flow due to the divergencies in future climate projection.

It is necessary to keep in mind that some natural and anthropogenic factors that could affect ARB hydrological processes were not included in this study. As this study intended to project river flow without much human intervention, river water diversion for irrigation and dam effect were not considered. We acknowledge that river water diversion and dam construction can strongly affect river flow, especially in the arid and semiarid regions (Kondolf and Batalla, 2005). If these factors are included, river flow reduction could be larger than our estimates.

Woody Plant Encroachment (WPE) into the arid and semiarid grasslands is a global phenomenon with critical hydrological consequences (e.g. Huxman et al., 2005; Qiao et al., 2015; Schreiner-McGraw et al., 2020; Zou et al., 2015). Compared to the original grasslands, WPE species have a higher transpiration, which reduces surface runoff and surface water availability. Eastern redcedar (juniper, Juniperus virginiana) and honey mesquite (mesquite, Prosopis glandulosa) are the two most common WPE species in the ARB and the southern Great Plains. In Oklahoma, juniper forests expand at a rate of 40 km<sup>2</sup>/year over recent decades (Wang et al., 2018). It is expected that woody plants will continue to encroach into the grasslands in the ARB in the future, but its expansion rate is subject to large uncertainties due to the changed climate conditions, fire regimes, and human willingness and management strategies to control WPE. If WPE impacts on ecosystem hydrological processes are considered, river flow in the ARB may be further reduced. Likewise, government policies on biofuels and tree planting for increased carbon storage are unknown factors related to future land-use change that may influence runoff and river flows. Our results in this study represent a conservative estimate of future river flow reduction.

Given the limitations in our study, we recommend the following future research directions. In the SSP2 and SSP5 scenarios, cropland area in the ARB will increase or keep stable at the current level, which is not consistent with the declining trend of cropland area in the U.S. and the Great Plains over recent decades (Yu and Lu, 2018). One future research direction is to include new land use change scenarios with continuously decreased cropland area to evaluate land use change impacts on regional water and other ecological processes. Dams, river water diversion, and woody plant encroachment are expected to change regional hydrological processes in the ARB but are not included in this study. We suggest future work to investigate to which extent human activities and woody plant encroachment would affect river flow. Additionally, it is necessary to examine the impacts of future river flow decline on the habitats of critical aquatic species and the reliability of water supply reservoirs.

## 5. Conclusions

In this study, we projected future river flow changes in the ARB using a process-based ecosystem model under two climate and socioeconomic scenarios. Our results showed that river flow in the ARB will decrease

significantly in the 21st century under both the SSP2-RCP45 and the SSP5-RCP85 scenarios. In the SSP2-RCP45, the river flow decline will take place from the beginning to the middle of this century. In the SSP5- RCP85, river flow decline will happen across the entire simulation priod. Compared to the period of 2000–2019, Arkansas river flow at the end of the 21st century will decrease by 12.1 % in the SSP2-RCP45 and 27.9 % in the SSP5-RCP85. Most importantly, river flow decline will happen in all the major rivers with the largest percentage reduction in the western and southwestern ARB. Climate warming and drying will be the primary factors accounting for this reduction. The reduced water availability and growing water demand will require conservative water use strategies and improved agricultural irrigation efficiency to maintain water resource sustainability.

#### **CRediT** authorship contribution statement

Jia Yang: Conceptualization, Methodology, Writing – original draft, Formal analysis, Writing – review & editing. Chris Zou: Conceptualization, Writing – original draft, Writing – review & editing. Rodney Will: Conceptualization, Writing – original draft, Writing – review & editing. Kevin Wagner: Writing – original draft, Funding acquisition, Writing – review & editing. Ying Ouyang: Writing – original draft, Funding acquisition, Writing – review & editing. Chad King: Writing – original draft, Writing – review & editing. Abigail Winrich: Writing – review & editing. Hanqin Tian: Methodology, Writing – original draft, Writing – review & editing.

## **Declaration of Competing Interest**

The authors declare that they have no known competing financial interests or personal relationships that could have appeared to influence the work reported in this paper.

## Data availability

Data will be made available on request.

## Acknowledgments

This work was supported by Oklahoma NSF EPSCoR S3OK project (award number: OIA-1946093), S3OK project Research Seed Grant, USDA McIntire-Stennis Grant (OKL03249, OKL03151, and OKL03152), and USDA Forest Service Agreement (21-JV-11330170-026). H.T. acknowledges funding support from NSF (grant number: 1903722). This work was partially supported by R.W.'s Sarkeys Distinguished Professorship.

## Data Statement

All the data used in this study can be downloaded from their respective websites. Historical and future climate were from gridMet climate data (https://www.northwestknowledge.net/metdata/data/) and the Multivariate Adaptive Constructed Analogs climate data (http://thredds.northwestknowledge.net:8080/thredds/reacch\_climate\_CMIP 5\_macav2\_catalog2.html). Contemporary land use and land cover data were from the National Land Cover Database (NLCD, https://s3-us-west-2.amazonaws.com/mrlc/

NLCD\_landcover\_2019\_release\_all\_files\_20210604.zip). Historical and future cropland distribution data were from Yu and Lu (2018) (https://doi.pangaea.de/10.1594/PANGAEA.881801) and the Land-Use Harmonization data (https://luh.umd.edu/data.shtml). CO2 data were from the NOAA Global Monitoring Laboratory (https://gml.noaa.gov/ ccgg/trends/data.html) and the RCP database version 2.0 (https:// tntcat.iiasa.ac.at/RcpDb/dsd?Action = htmlpage&page = download).

Atmospheric nitrogen deposition data were from the NCAR Chemistry-Climate Model Initiative (CCMI), available at https://data.isimip.org/search/subcategory/n-deposition/product/InputData/. Soil properties data were from the gridded Harmonized World Soil Database (HWSD) v1.2 (https://daac.ornl.gov/SOILS/guides/HWSD.html). Topography

and river network were developed according to Digital Elevation Model in the Hydro1k and GTOPO30, which can be downloaded from USGS EarthExplorer (https://earthexplorer.usgs.gov/). Regional evapotranspiration datasets for model validatation and comparison were from the product of Model Tree Ensembles (https://www. bgc-jena.mpg.de/geodb/projects/Data.php), ET estimates from the Global Land Evaporation Amsterdam Model (GLEAM, https://www. gleam.eu/, registration is needed), and MODIS ET product of MOD16A3 (accessible through USGS AppEEARS tool, https://lpdaac.usgs.gov/tools/appeears/).

River flow measurements were downloaded from USGS Surface- Water Monthly Statistics (https://waterdata.usgs.gov/nwis/monthly/? referred\_module = sw).

## Appendix A. Supplementary data

Supplementary data to this article can be found online at https://doi.org/10.1016/j.jhydrol.2023.129253.

#### References

- Abatzoglou, J.T., 2013. Development of gridded surface meteorological data for ecological applications and modelling. Int. J. Climatol. 33, 121–131. https://doi.org/10.1002/joc.3413.
- Abatzoglou, J.T., Brown, T.J., 2012. A comparison of statistical downscaling methods suited for wildfire applications. Int. J. Climatol. 32, 772–780. https://doi.org/10.1002/joc.2312.
- Acharya, B.S., Kharel, G., Zou, C.B., Wilcox, B.P., Halihan, T., 2018. Woody Plant Encroachment Impacts on Groundwater Recharge: A Review. Water 10, 1466. https://doi.org/10.3390/w10101466.
- Ainsworth, E.A., Long, S.P., 2005. What have we learned from 15 years of free-air CO2 enrichment (FACE)? A meta-analytic review of the responses of photosynthesis, canopy properties and plant production to rising CO2. New Phytol. 165, 351–372. https://doi.org/10.1111/j.1469-8137.2004.01224.x.
- Ainsworth, E.A., Rogers, A., 2007. The response of photosynthesis and stomatal conductance to rising [CO2]: mechanisms and environmental interactions. Plant Cell Environ. 30, 258–270. https://doi.org/10.1111/j.1365-3040.2007.01641.x.
- Ali, R., Kuriqi, A., Abubaker, S., Kisi, O., 2019. Long-Term Trends and Seasonality

  Detection of the Observed Flow in Yangtze River Using Mann-Kendall and Sen's
  Innovative Trend Method. Water 11, 1855. https://doi.org/10.3390/w11091855.
- Almazroui, M., Islam, M.N., Saeed, F., Saeed, S., Ismail, M., Ehsan, M.A., Diallo, I., O'Brien, E., Ashfaq, M., Martínez-Castro, D., Cavazos, T., Cerezo-Mota, R., Tippett, M.K., Gutowski, W.J., Alfaro, E.J., Hidalgo, H.G., Vichot-Llano, A., Campbell, J.D., Kamil, S., Rashid, I.U., Sylla, M.B., Stephenson, T., Taylor, M., Barlow, M., 2021. Projected Changes in Temperature and Precipitation Over the United States, Central America, and the Caribbean in CMIP6 GCMs. Earth Syst. Environ. 5, 1–24. https://doi.org/10.1007/s41748-021-00199-5.
- Basara, J.B., Christian, J.I., Wakefield, R.A., Otkin, J.A., Hunt, E.H., Brown, D.P., 2019. The evolution, propagation, and spread of flash drought in the Central United States during 2012. Environ. Res. Lett. 14, 084025 https://doi.org/10.1088/1748-9326/ab2cc0.
- Basara, J.B., Maybourn, J.N., Peirano, C.M., Tate, J.E., Brown, P.J., Hoey, J.D., Smith, B. R., 2013. Drought and Associated Impacts in the Great Plains of the United States—A Review 2013. https://doi.org/10.4236/ijg.2013.46A2009.
- Budyko, M.I., 1951. On climatic factors of runoff (in Russian). Probl. Fiz Geogr. 16, 41–48.
- Cepeda, J., 2016. History of Lake Meredith inflows and lake levels, 1965 2015. Presented at the GSA Annual Meeting, Geological Society of America, Denver, Colorado. Doi: 10.1130/abs/2016AM-278534.
- Chen, L.G., Gottschalck, J., Hartman, A., Miskus, D., Tinker, R., Artusa, A., 2019. Flash Drought Characteristics Based on U.S. Drought Monitor. Atmosphere 10, 498. https://doi.org/10.3390/atmos10090498.
- Chen, G., Tian, H., Huang, C., Prior, S.A., Pan, S., 2013. Integrating a process-based ecosystem model with Landsat imagery to assess impacts of forest disturbance on terrestrial carbon dynamics: Case studies in Alabama and Mississippi. J. Geophys.
  Res. Biogeosciences 118, 1208–1224. https://doi.org/10.1002/jgrg.20098.
- Christian, J.I., Basara, J.B., Otkin, J.A., Hunt, E.D., Wakefield, R.A., Flanagan, P.X., Xiao, X., 2019. A Methodology for Flash Drought Identification: Application of Flash Drought Frequency across the United States. J. Hydrometeorol. 20, 833–846.

https://doi.org/10.1175/JHM-D-18-0198.1.

- Clemons, J., 2003. Interstate water disputes: A road map for states. Southeast. Environ. Law J. 12, 115.
- Dangal, S.R.S., Tian, H., Lu, C., Ren, W., Pan, S., Yang, J., Di Cosmo, N., Hessl, A., 2017. Integrating Herbivore Population Dynamics Into a Global Land Biosphere Model: Plugging Animals Into the Earth System. J. Adv. Model. Earth Syst. 9, 2920–2945. https://doi.org/10.1002/2016MS000904.
- Dickinson, R.E., Berry, J.A., Bonan, G.B., Collatz, G.J., Field, C.B., Fung, I.Y., Goulden, M., Hoffmann, W.A., Jackson, R.B., Myneni, R., Sellers, P.J., Shaikh, M., 2002. Nitrogen Controls on Climate Model Evapotranspiration. J. Clim. 15, 278–295. https://doi.org/10.1175/1520-0442(2002)015<0278:NCOCME>2.0.CO;2.

- Djokic, D., Ye, Z., Dartiguenave, C., 2011. Arc hydro tools overview. Redland Can, ESRI, p. 5.
- Evett, S.R., Colaizzi, P.D., Lamm, F.R., O'Shaughnessy, S.A., Heeren, D.M., Trout, T.J., Kranz, W.L., Lin, X., 2020. Past, present, and future of irrigation on the US Great Plains. Trans. ASABE 63, 703–729
- Gates, T.K., Steed, G.H., Niemann, J.D., Labadie, J.W., 2016. Data for improved water management in Colorado's Arkansas River Basin: hydrological and water quality studies.

  State Univ. Fort Collins. Colo. Colorado. Colorado Water Institute Special Report No. 24.
- Gedney, N., Cox, P.M., Betts, R.A., Boucher, O., Huntingford, C., Stott, P.A., 2006. Detection of a direct carbon dioxide effect in continental river runoff records. Nature 439, 835–838. https://doi.org/10.1038/nature04504.
- Gilliam, F.S., Burns, D.A., Driscoll, C.T., Frey, S.D., Lovett, G.M., Watmough, S.A., 2019. Decreased atmospheric nitrogen deposition in eastern North America: Predicted responses of forest ecosystems. Environ. Pollut. 244, 560–574. https://doi.org/10.1016/j.envpol.2018.09.135.
- Gu, Z., Qi, Z., Burghate, R., Yuan, S., Jiao, X., Xu, J., 2020. Irrigation Scheduling Approaches and Applications: A Review. J. Irrig. Drain. Eng. 146, 04020007. https://doi.org/10.1061/(ASCE)JR.1943-4774.0001464.
- Gupta, H.V., Sorooshian, S., Yapo, P.O., 1999. Status of Automatic Calibration for Hydrologic Models: Comparison with Multilevel Expert Calibration. J. Hydrol. Eng. 4, 135–143. https://doi.org/10.1061/(ASCE)1084-0699(1999)4:2(135).
- Homer, C., Dewitz, J., Jin, S., Xian, G., Costello, C., Danielson, P., Gass, L., Funk, M., Wickham, J., Stehman, S., Auch, R., Riitters, K., 2020. Conterminous United States land cover change patterns 2001–2016 from the 2016 National Land Cover Database. ISPRS J. Photogramm. Remote Sens. 162, 184–199. https://doi.org/10.1016/j.isprsjprs.2020.02.019.
- Hurtt, G.C., Chini, L., Sahajpal, R., Frolking, S., Bodirsky, B.L., Calvin, K., Doelman, J.C., Fisk, J., Fujimori, S., Klein Goldewijk, K., Hasegawa, T., Havlik, P., Heinimann, A., Humpenoder, F., Jungclaus, J., Kaplan, J.O., Kennedy, J., Krisztin, T., Lawrence, D., "Lawrence, P., Ma, L., Mertz, O., Pongratz, J., Popp, A., Poulter, B., Riahi, K., Shevliakova, E., Stehfest, E., Thornton, P., Tubiello, F.N., van Vuuren, D.P., Zhang, X., 2020. Harmonization of global land use change and management for the period 850–2100 (LUH2) for CMIP6. Geosci. Model Dev. 13, 5425–5464. https://doi.org/10.5194/gmd-13-5425-2020.
- Huxman, T.E., Wilcox, B.P., Breshears, D.D., Scott, R.L., Snyder, K.A., Small, E.E., Hultine, K., Pockman, W.T., Jackson, R.B., 2005. Ecohydrological Implications of Woody Plant Encroachment. Ecology 86, 308–319. https://doi.org/10.1890/03-0583.
- Jung, M., Reichstein, M., Ciais, P., Seneviratne, S.I., Sheffield, J., Goulden, M.L., Bonan, G., Cescatti, A., Chen, J., de Jeu, R., Dolman, A.J., Eugster, W., Gerten, D., Gianelle, D., Gobron, N., Heinke, J., Kimball, J., Law, B.E., Montagnani, L., Mu, Q., Mueller, B., Oleson, K., Papale, D., Richardson, A.D., Roupsard, O., Running, S., Tomelleri, E., Viovy, N., Weber, U., Williams, C., Wood, E., Zaehle, S., Zhang, K., 2010. Recent decline in the global land evapotranspiration trend due to limited moisture supply. Nature 467, 951–954. https://doi.org/10.1038/nature09396.
- Jung, M., Reichstein, M., Margolis, H.A., Cescatti, A., Richardson, A.D., Arain, M.A., Arneth, A., Bernhofer, C., Bonal, D., Chen, J., Gianelle, D., Gobron, N., Kiely, G., Kutsch, W., Lasslop, G., Law, B.E., Lindroth, A., Merbold, L., Montagnani, L., Moors, E.J., Papale, D., Sottocornola, M., Vaccari, F., Williams, C., 2011. Global patterns of land-atmosphere fluxes of carbon dioxide, latent heat, and sensible heat derived from eddy covariance, satellite, and meteorological observations.
- J. Geophys. Res. Biogeosciences 116. https://doi.org/10.1029/2010JG001566. Kenny, J.F., 2014. Public-supply water use in Kansas, 1990–2012 (Fact SheU.S. Geological Survey Fact Sheetet No. 3116). Fact Sheet.
- Khan, S., Anwar, S., Yu, S., Sun, M., Yang, Z., Gao, Z., 2019. Development of Drought- Tolerant Transgenic Wheat: Achievements and Limitations. Int. J. Mol. Sci. 20, 3350. https://doi.org/10.3390/ijms20133350.
- Kondolf, G., Batalla, R.J., 2005. Chapter 11 Hydrological effects of dams and water diversions on rivers of Mediterranean-climate regions: examples from California, in: Garcia, C., Batalla, R.J. (Eds.), Developments in Earth Surface Processes, Catchment Dynamics and River Processes. Elsevier, pp. 197–211. Doi: 10.1016/S0928-2025(05) 80017-3.
- Krause, A., Haverd, V., Poulter, B., Anthoni, P., Quesada, B., Rammig, A., Arneth, A., 2019. Multimodel Analysis of Future Land Use and Climate Change Impacts on Ecosystem Functioning. Earths Future 7, 833–851. https://doi.org/10.1029/2018EF001123.
- Lamm, F.R., Bordovsky, J.P., Schwankl, L.J., Grabow, G.L., Enciso-Medina, J., Peters, R. T., Colaizzi, P.D., Trooien, T.P., Porter, D.O., 2012. Subsurface drip irrigation: Status of the technology in 2010. Trans. ASABE 55, 483–491.
- Lauri, H., de Moel, H., Ward, P.J., Ras" anen, T.A., Keskinen, M., Kummu, M., 2012. Future "changes in Mekong River hydrology: impact of climate change and reservoir operation on discharge. Hydrol. Earth Syst. Sci. 16, 4603–4619. https://doi.org/ 10.5194/hess-16-4603-2012.
- Lee, M., Tansel, B., Balbin, M., 2013. Urban Sustainability Incentives for Residential Water Conservation: Adoption of Multiple High Efficiency Appliances. Water Resour. Manag. 27, 2531–2540. https://doi.org/10.1007/s11269-013-0301-8.
- Levidow, L., Zaccaria, D., Maia, R., Vivas, E., Todorovic, M., Scardigno, A., 2014. Improving water-efficient irrigation: Prospects and difficulties of innovative practices. Agric. Water Manag. 146. 84–94. https://doi.org/10.1016/j. agwat.2014.07.012.
- Li, D., Pan, M., Cong, Z., Zhang, L., Wood, E., 2013. Vegetation control on water and energy balance within the Budyko framework. Water Resour. Res. 49, 969–976. https://doi.org/10.1002/wrcr.20107.
- Liu, M., Adam, J.C., Richey, A.S., Zhu, Z., Myneni, R.B., 2018. Factors controlling changes in evapotranspiration, runoff, and soil moisture over the conterminous U.S.: Accounting for vegetation dynamics. J. Hydrol. 565, 123–137. https://doi.org/10.1016/j.jhydrol.2018.07.068.
- Liu, L., Hong, Y., Looper, J., Riley, R., Yong, B., Zhang, Z., Hocker, J., Shafer, M., 2013a.

  Climatological Drought Analyses and Projection Using SPI and PDSI: Case Study of the

- Arkansas Red River Basin. J. Hydrol. Eng. 18, 809–816. https://doi.org/10.1061/(ASCE)HE.1943-5584.0000619.
- Liu, M., Tian, H., Yang, Q., Yang, J., Song, X., Lohrenz, S.E., Cai, W.-J., 2013b. Long-term trends in evapotranspiration and runoff over the drainage basins of the Gulf of Mexico during 1901– 2008. Water Resour. Res. 49. 1988–2012. https://doi.org/10.1002/wrcr.20180.
- Livneh, B., Hoerling, M.P., 2016. The Physics of Drought in the U.S Central Great Plains. J. Clim. 29, 6783–6804. https://doi.org/10.1175/JCLI-D-15-0697.1.
- Lu, C., Zhang, J., Tian, H., Crumpton, W.G., Helmers, M.J., Cai, W.-J., Hopkinson, C.S., Lohrenz, S.E., 2020. Increased extreme precipitation challenges nitrogen load management to the Gulf of Mexico. Commun. Earth Environ. 1, 1–10. https://doi. org/10.1038/s43247-020-00020-7.
- Maggioni, E., 2015. Water demand management in times of drought: What matters for water conservation. Water Resour. Res. 51, 125–139. https://doi.org/10.1002/2014WR016301.
- Mansur, E.T., Olmstead, S.M., 2012. The value of scarce water: Measuring the inefficiency of municipal regulations. J. Urban Econ. 71, 332–346. https://doi.org/ 10.1016/i.jue.2011.11.003.
- Mao, J., Fu, W., Shi, X., Ricciuto, D.M., Fisher, J.B., Dickinson, R.E., Wei, Y., Shem, W., Piao, S., Wang, K., Schwalm, C.R., Tian, H., Mu, M., Arain, A., Ciais, P., Cook, R., Dai, Y., Hayes, D., Hoffman, F.M., Huang, M., Huang, S., Huntzinger, D.N., Ito, A., Jain, A., King, A.W., Lei, H., Lu, C., Michalak, A.M., Parazoo, N., Peng, C., Peng, S., Poulter, B., Schaefer, K., Jafarov, E., Thornton, P.E., Wang, W., Zeng, N., Zeng, Z., Zhao, F., Zhu, Q., Zhu, Z., 2015. Disentangling climatic and anthropogenic controls on global terrestrial evapotranspiration trends. Environ. Res. Lett. 10, 094008 https://doi.org/10.1088/1748-9326/10/9/094008.
- Martens, B., Miralles, D.G., Lievens, H., van der Schalie, R., de Jeu, R.A.M., Fernandez- Prieto, D., Beck, H.E., Dorigo, W.A., Verhoest, N.E.C., 2017. GLEAM v3: satellite- based land evaporation and root-zone soil moisture. Geosci. Model Dev. 10, 1903–1925. https://doi.org/10.5194/gmd-10-1903-2017.
- Middleton, N., Thomas, D., 1998. World atlas of desertification.. ed. 2. Arnold, Hodder Headline, PLC.
- Moriasi, D., Arnold, J., Van Liew, M., Bingner, R., Harmel, R., Veith, T., 2007. Model Evaluation Guidelines for Systematic Quantification of Accuracy in Watershed Simulations. Trans. ASABE 50, 885–900. https://doi.org/10.13031/2013.23153.
- Mu, Q., Zhao, M., Running, S.W., 2011. Improvements to a MODIS global terrestrial evapotranspiration algorithm. Remote Sens. Environ. 115, 1781–1800. https://doi. org/10.1016/j.rse.2011.02.019.
- Naeser, R.B., Bennett, L.L., 1998. The cost of noncompliance: The economic value of water in the Middle Arkansas River Valley. Nat. Resour. J. 445–463.
- Nash, J.E., Sutcliffe, J.V., 1970. River flow forecasting through conceptual models part I — A discussion of principles. J. Hydrol. 10, 282–290. https://doi.org/10.1016/0022-1694(70)90255-6.
- Nohara, D., Kitoh, A., Hosaka, M., Oki, T., 2006. Impact of Climate Change on River Discharge Projected by Multimodel Ensemble. J. Hydrometeorol. 7, 1076–1089. https://doi.org/10.1175/JHM531.1.
- Olmstead, S.M., Stavins, R.N., 2009. Comparing price and nonprice approaches to urban water conservation. Water Resour. Res. 45 https://doi.org/10.1029/ 2008WR007227.
- Ortiz, R.F., Lewis, M.E., Radell, M.J., 1998. Water-quality Assessment of the Arkansas River Basin, Southeastern Colorado, 1990-93 (USGS Numbered Series No. 97–4111), Water-Resources Investigations Report. US Department of the Interior, US Geological Survey.
- Palmer, M.A., Reidy Liermann, C.A., Nilsson, C., Florke, M., Alcamo, J., Lake, P.S., "Bond, N., 2008. Climate change and the world's river basins: anticipating management options. Front. Ecol. Environ. 6. 81–89. https://doi.org/10.1890/060148.
- Pan, S., Tian, H., Dangal, S.R.S., Yang, Q., Yang, J., Lu, C., Tao, B., Ren, W., Ouyang, Z., 2015.

  Responses of global terrestrial evapotranspiration to climate change and increasing atmospheric CO2 in the 21st century. Earths Future 3, 15–35. https://doi.org/10.1002/2014EF000263.
- Pan, S., Yang, J., Tian, H., Shi, H., Chang, J., Ciais, P., Francois, L., Frieler, K., Fu, B., Hickler, T., Ito, A., Nishina, K., Ostberg, S., Reyer, C.P.O., Schaphoff, S., Steinkamp, J., Zhao, F., 2020. Climate Extreme Versus Carbon Extreme: Responses of Terrestrial Carbon Fluxes to Temperature and Precipitation. J. Geophys. Res. Biogeosciences 125. https://doi.org/10.1029/2019JG005252.
- Pan, S., Bian, Z., Tian, H., Yao, Y., Najjar, R.G., Friedrichs, M.A.M., Hofmann, E.E., Xu, R., Zhang, B., 2021. Impacts of Multiple Environmental Changes on Long-Term Nitrogen Loading From the Chesapeake Bay Watershed. J. Geophys. Res. Biogeosci. 126 https://doi.org/10.1029/2020JG005826.
- Piao, S., Friedlingstein, P., Ciais, P., de Noblet-Ducoudr'e, N., Labat, D., Zaehle, S., 2007. Changes in climate and land use have a larger direct impact than rising CO2 on global river runoff trends. Proc. Natl. Acad. Sci. 104, 15242–15247. https://doi.org/ 10.1073/pnas.0707213104
- Pigg, J., 1999. Decreasing abundance of the Arkansas River shiner in the South Canadian River, Oklahoma, in: Proceedings of the Oklahoma Academy of Science. pp. 7–12.
- Popp, A., Calvin, K., Fujimori, S., Havlik, P., Humpenoder, F., Stehfest, E., Bodirsky, B.L., "Dietrich, J.P., Doelmann, J.C., Gusti, M., Hasegawa, T., Kyle, P., Obersteiner, M., Tabeau, A., Takahashi, K., Valin, H., Waldhoff, S., Weindl, I., Wise, M., Kriegler, E., Lotze-Campen, H., Fricko, O., Riahi, K., van Vuuren, D.P., 2017. Land-use futures in the shared socio-economic pathways. Glob. Environ. Change 42, 331–345. https://doi.org/10.1016/j.gloenycha.2016.10.002.
- Qiao, L., Zou, C.B., Will, R.E., Stebler, E., 2015. Calibration of SWAT model for woody plant encroachment using paired experimental watershed data. J. Hydrol. 523, 231–239. https://doi.org/10.1016/j.jhydrol.2015.01.056.

- Qiao, L., Zou, C.B., Stebler, E., Will, R.E., 2017. Woody plant encroachment reduces annual runoff and shifts runoff mechanisms in the tallgrass prairie, USA. Water Resour. Res. 53, 4838–4849. https://doi.org/10.1002/2016WR019951.
- Ren, W., Tian, H., Cai, W.-J., Lohrenz, S.E., Hopkinson, C.S., Huang, W.-J., Yang, J., Tao, B., Pan, S., He, R., 2016. Century-long increasing trend and variability of dissolved organic carbon export from the Mississippi River basin driven by natural and anthropogenic forcing. Glob. Biogeochem. Cycles 30, 1288–1299. https://doi.org/10.1002/2016GB005395.
- Rogers, D.H., Lamm, F.R., 2008. Kansas irrigation trends, in: Proceedings of the 2012 Central Plains Irrigation Conference, Colby, Kansas, February 21-22. Colorado State University. Libraries.
- Scheff, J., Frierson, D.M.W., 2014. Scaling Potential Evapotranspiration with Greenhouse Warming. J. Clim. 27, 1539–1558. https://doi.org/10.1175/JCLI-D-13-00233.1.
- Schilling, K.E., Chan, K.-S., Liu, H., Zhang, Y.-K., 2010. Quantifying the effect of land use land cover change on increasing discharge in the Upper Mississippi River. J. Hydrol. 387, 343–345. https://doi.org/10.1016/j.jhydrol.2010.04.019.
- Schlager, E., Heikkila, T., 2009. Resolving Water Conflicts: A Comparative Analysis of Interstate River Compacts. Policy Stud. J. 37, 367–392. https://doi.org/10.1111/j.1541-0072.2009.00319.x.
- Schreiner-McGraw, A.P., Vivoni, E.R., Ajami, H., Sala, O.E., Throop, H.L., Peters, D.P.C., 2020. Woody Plant Encroachment has a Larger Impact than Climate Change on Dryland Water Budgets. Sci. Rep. 10, 8112. https://doi.org/10.1038/s41598-020-65094-x.
- Schubert, S.D., Suarez, M.J., Pegion, P.J., Koster, R.D., Bacmeister, J.T., 2004. Causes of Long-Term Drought in the U.S. Great Plains. J. Clim. 17, 485–503. https://doi.org/ 10.1175/1520-0442(2004)017<0485:COLDIT>2.0.CO:2.
- Seager, R., Ting, M., Li, C., Naik, N., Cook, B., Nakamura, J., Liu, H., 2013. Projections of declining surface-water availability for the southwestern United States. Nat. Clim. Change 3, 482–486. https://doi.org/10.1038/nclimate1787.
- Shi, X., Mao, J., Thornton, P.E., Huang, M., 2013. Spatiotemporal patterns of evapotranspiration in response to multiple environmental factors simulated by the Community Land Model. Environ. Res. Lett. 8, 024012 https://doi.org/10.1088/1748-9326/8/2/024012.
- Shi, H., Tian, H., Pan, N., Reyer, C.P.O., Ciais, P., Chang, J., Forrest, M., Frieler, K., Fu, B., Gadeke, A., Hickler, T., Ito, A., Ostberg, S., Pan, S., Stevanovi 'c, M., Yang, J., 2021.
  Saturation of Global Terrestrial Carbon Sink Under a High Warming Scenario. Glob. Biogeochem. Cycles 35. https://doi.org/10.1029/2020GB006800.
- Siriwardena, L., Finlayson, B.L., McMahon, T.A., 2006. The impact of land use change on catchment hydrology in large catchments: The Comet River, Central Queensland. Australia. J. Hydrol. 326, 199–214. https://doi.org/10.1016/j.jhydrol.2005.10.030.
- Still, C.J., Berry, J.A., Collatz, G.J., DeFries, R.S., 2003. Global distribution of C3 and C4 vegetation: Carbon cycle implications. Glob. Biogeochem. Cycles 17. https://doi. org/10.1029/2001GB001807.
- Tao, B., Tian, H., Ren, W., Yang, J., Yang, Q., He, R., Cai, W., Lohrenz, S., 2014. Increasing Mississippi river discharge throughout the 21st century influenced by changes in climate, land use, and atmospheric CO2. Geophys. Res. Lett. 41, 4978–4986. https://doi.org/10.1002/2014GL060361.
- Taylor, K.E., Stouffer, R.J., Meehl, G.A., 2012. An Overview of CMIP5 and the Experiment Design. Bull. Am. Meteorol. Soc. 93, 485–498. https://doi.org/10.1175/BAMS-D-11-00094.1.
- Thrasher, B., Nemani, R., 2021. NASA Earth Exchange Global Daily Downscaled Projections (NEX-GDDP-CMIP6).
- Tian, H., Chen, G., Liu, M., Zhang, C., Sun, G., Lu, C., Xu, X., Ren, W., Pan, S., Chappelka, A., 2010. Model estimates of net primary productivity, evapotranspiration, and water use efficiency in the terrestrial ecosystems of the southern United States during 1895–2007. For. Ecol. Manag., Managing landscapes at multiple scales for sustainability of ecosystem functions 259, 1311–1327. Doi: 10.1016/j. foreco.2009.10.009.
- Tian, H., Xu, X., Lu, C., Liu, M., Ren, W., Chen, G., Melillo, J., Liu, J., 2011. Net exchanges of CO2, CH4, and N2O between China's terrestrial ecosystems and the atmosphere and their contributions to global climate warming. J. Geophys. Res. Biogeosciences 116. https://doi.org/10.1029/2010JG001393.
- Tian, H., Yang, J., Lu, C., Xu, R., Canadell, J.G., Jackson, R.B., Arneth, A., Chang, J., Chen, G., Ciais, P., Gerber, S., Ito, A., Huang, Y., Joos, F., Lienert, S., Messina, P., Olin, S., Pan, S., Peng, C., Saikawa, E., Thompson, R.L., Vuichard, N., Winiwarter, W., Zaehle, S., Zhang, B., Zhang, K., Zhu, Q., 2018. The Global N2O Model Intercomparison Project. Bull. Am. Meteorol. Soc. 99, 1231–1251. https:// doi.org/10.1175/BAMS-D-17-0212.1.
- Tian, H., Xu, R., Pan, S., Yao, Y., Bian, Z., Cai, W.-J., Hopkinson, C.S., Justic, D., Lohrenz, S., Lu, C., Ren, W., Yang, J., 2020. Long-Term Trajectory of Nitrogen Loading and Delivery From Mississippi River Basin to the Gulf of Mexico. Glob. Biogeochem. Cycles 34. https://doi.org/10.1029/2019GB006475.
- Tortorelli, R.L., 2009. Water Use in Oklahoma 1950–2005 (USGS Scientific- Investigations Report No. 5212).
- Tosunoglu, F., Kisi, O., 2017. Trend Analysis of Maximum Hydrologic Drought Variables Using Mann-Kendall and S,en's Innovative Trend Method. River Res. Appl. 33, 597–610. https://doi.org/10.1002/rra.3106. van Vliet, M.T.H., Franssen, W.H.P., Yearsley, J.R., Ludwig, F., Haddeland, I., Lettenmaier, D.P., Kabat, P., 2013. Global river discharge and water temperature under climate change. Glob. Environ. Change 23, 450–464. https://doi.org/10.1016/j.gloenycha.2012.11.002.
- Velpuri, N.M., Senay, G.B., Singh, R.K., Bohms, S., Verdin, J.P., 2013. A comprehensive evaluation of two MODIS evapotranspiration products over the conterminous United States: Using point and gridded FLUXNET and water balance ET. Remote Sens. Environ. 139, 35–49. https://doi.org/10.1016/j.rse.2013.07.013.
- Vor osmarty, C.J., Green, P., Salisbury, J., Lammers, R.B., 2000. Global Water Resources: Vulnerability from Climate Change and Population Growth. Science 289, 284–288. https://doi.org/10.1126/science.289.5477.284.

- Wang, J., Xiao, X., Qin, Y., Doughty, R.B., Dong, J., Zou, Z., 2018. Characterizing the encroachment of juniper forests into sub-humid and semi-arid prairies from 1984 to 2010 using PALSAR and Landsat data. Remote Sens. Environ. 205, 166–179. https://doi.org/10.1016/j.rse.2017.11.019.
- Ward, F.A., Pulido-Velazquez, M., 2008. Water conservation in irrigation can increase water use. Proc. Natl. Acad. Sci. 105, 18215–18220. https://doi.org/10.1073/pnas.0805554105.
- Wichman, C.J., Taylor, L.O., von Haefen, R.H., 2016. Conservation policies: Who responds to price and who responds to prescription? J. Environ. Econ. Manag. 79, 114–134. https://doi.org/10.1016/j.jeem.2016.07.001.
- Wieder, W., 2014. Regridded Harmonized World Soil Database v1.2 59.234908 MB. https://doi.org/10.3334/ORNLDAAC/1247.
- Yang, J., Tian, H., Tao, B., Ren, W., Lu, C., Pan, S., Wang, Y., Liu, Y., 2015a. Century-scale patterns and trends of global pyrogenic carbon emissions and fire influences on terrestrial carbon balance. Glob. Biogeochem. Cycles 29, 1549–1566. https://doi. org/10.1002/2015GB005160.
- Yang, J., Ren, W., Ouyang, Y., Feng, G., Tao, B., Granger, J.J., Poudel, K.P., 2019a. Projection of 21st century irrigation water requirement across the Lower Mississippi Alluvial Valley. Agric. Water Manag. 217, 60–72. https://doi.org/10.1016/j.agwat.2019.02.033.
- Yang, Q., Tian, H., Friedrichs, M.A.M., Liu, M., Li, X., Yang, J., 2015b. Hydrological Responses to Climate and Land-Use Changes along the North American East Coast: A 110-Year Historical Reconstruction. JAWRA J. Am. Water Resour. Assoc. 51, 47–67. https://doi.org/10.1111/jawr.12232.
- Yang, Z., Zhang, Q., Hao, X., Yue, P., 2019b. Changes in Evapotranspiration Over Global Semiarid Regions 1984–2013. J. Geophys. Res. Atmospheres 124, 2946–2963. https://doi.org/10.1029/2018JD029533.
- Yao, Y., Tian, H., Shi, H., Pan, S., Xu, R., Pan, N., Canadell, J.G., 2020. Increased global nitrous oxide emissions from streams and rivers in the Anthropocene. Nat. Clim. Change 10, 138–142. https://doi.org/10.1038/s41558-019-0665-8.
- Yu, Z., Lu, C., 2018. Historical cropland expansion and abandonment in the continental U.S. during 1850 to 2016. Glob. Ecol. Biogeogr. 27, 322–333. https://doi.org/ 10.1111/geb.12697.
- Yue, S., Wang, C., 2004. The Mann-Kendall Test Modified by Effective Sample Size to Detect Trend in Serially Correlated Hydrological Series. Water Resour. Manag. 18, 201–218. https://doi.org/10.1023/B:WARM.0000043140.61082.60.
- Yue, P., Zhang, Q., Ren, X., Yang, Z., Li, H., Yang, Y., 2022. Environmental and biophysical effects of evapotranspiration in semiarid grassland and maize cropland ecosystems over the summer monsoon transition zone of China. Agric. Water Manag. 264, 107462 https://doi.org/10.1016/j.agwat.2022.107462.
- Zhang, Y.-K., Schilling, K.E., 2006. Increasing streamflow and baseflow in Mississippi River since the 1940s: Effect of land use change. J. Hydrol. 324, 412–422. https://doi.org/10.1016/j.jhydrol.2005.09.033.
- Zou, C.B., Caterina, G.L., Will, R.E., Stebler, E., Turton, D., 2015. Canopy Interception for a Tallgrass Prairie under Juniper Encroachment. PLOS ONE 10, e0141422.